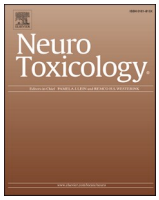
Neurotoxicology 117 (2026) 103580



Contents lists available at ScienceDirect

Neurotoxicology

journal homepage: www.elsevier.com/locate/neuro



APOE genotype shapes persistent behavioral and molecular alterations following early postnatal particulate matter exposure in humanized apoE3 and apoE4 mice

Rocío Rodulfo-Cárdenas [a,b,c,d], Judit Biosca-Brull [a,c,d,e], Séfora Barberà-Parada [a,b,c,d], Raquel Gabaldón-Díaz [a,c,d,e], Diego Ruiz-Sobremazas [f,g], Jordi Blanco [a,c,d,h], Maria Cabré [a,d,e], José L. Domingo [i], Caridad López-Granero [g], Fernando Sánchez-Santed [f], Maria Teresa Colomina [a,b,c,d,*]

[a] Universitat Rovira i Virgili, Research Group in Neurobehavior and Health (NEUROLAB), Tarragona, Spain
[b] Universitat Rovira i Virgili, Department of Psychology and Research Center for Behavior Assessment (CRAMC), Tarragona, Spain
[c] Universitat Rovira i Virgili, The Environmental, Food and Toxicology Technology Center (TecnATox), Reus, Spain
[d] Institut de Recerca Biomèdica Catalunya Sud (IRB CatSud), Tarragona, Spain
[e] Universitat Rovira i Virgili, Department of Biochemistry and Biotechnology, Tarragona, Spain
[f] Department of Psychology and CIBIS, University of Almeria, Almeria, Spain
[g] University of Zaragoza, Department of Psychology and Sociology, Teruel, Spain
[h] Universitat Rovira i Virgili, Department of Basic Medical Sciences, Reus, Spain
[i] Universitat Rovira i Virgili, Laboratory of Toxicology and Environmental Health, School of Medicine, Reus, Spain

ARTICLE INFO

Edited by Dr. P Lein and Dr. R Westerink

Keywords:
Particulate matter
APOE genotype
Neurodevelopment
Air pollution
Behavior
Gene expression
Gene-environment interaction

ABSTRACT

Early-life exposure to particulate matter (PM) can interfere with brain maturation and has been linked to persistent neurobehavioral alterations. However, individual susceptibility is likely influenced by both genetic background and biological sex. *APOE* is particularly relevant in this context because its ε4 allele is associated with altered neuroimmune, synaptic, metabolic, and stress-related responses that may modify vulnerability to environmental insults. Here, we investigated whether early postnatal PM exposure produces persistent behavioral and molecular alterations in young adult male and female humanized apoE3 and apoE4 targeted-replacement mice. Mice were exposed by whole-body inhalation to Fine Atmospheric PM (SRM 2787, NIST) or saline for 1 h/day from postnatal day (PND) 4 to PND14, using an exposure paradigm designed to achieve a nominal theoretical maximum chamber concentration of 3789 μg/m^3. Nevertheless, the actual airborne concentration was not directly measured. Behavioral testing was performed from PND50 to PND96, followed by hippocampal and striatal gene-expression analyses. Early postnatal PM exposure produced selective rather than generalized neurotoxic effects. *APOE* genotype emerged as the main determinant of adult behavioral and transcriptional profiles, with apoE4 mice showing a more anxiety-like behavioral profile and hippocampal transcriptional reorganization involving synaptic, glutamatergic, glial, myelin-related, redox, and stress-response pathways. PM exposure produced subtle social-behavior effects and suggested potential sex- and region-dependent modulation of glutamatergic and stress-related molecular markers. Overall, *APOE* genotype strongly shaped adult behavioral and transcriptional profiles, whereas PM effects varied by genotype, sex, and brain region, supporting *APOE*-dependent neurodevelopmental trajectories as modulators of persistent brain responses to early-life air-pollution exposure.

1. Introduction

Air pollution (AP) is currently considered one of the leading environmental risk factors for human health worldwide (Cohen et al., 2017), with most of the global population exposed to concentrations exceeding WHO air quality guideline (AQG) values (WHO, 2021).

* Corresponding author at: Universitat Rovira i Virgili, Research Group in Neurobehavior and Health (NEUROLAB), Tarragona, Spain.
E-mail address: mariateresa.colomina@urv.cat (M.T. Colomina).

https://doi.org/10.1016/j.neuro.2026.103580
Received 2 July 2026; Received in revised form 1 September 2026; Accepted 21 September 2026
Available online 24 September 2026
0161-813X/© 2026 The Author(s). Published by Elsevier B.V. This is an open access article under the CC BY-NC-ND license (http://creativecommons.org/licenses/by-nc-nd/4.0/).

Among airborne pollutants, particulate matter (PM) has received particular attention due to its well-established association with cardiovascular, respiratory, and metabolic disorders (Feng et al., 2016). Inhalation is the primary route of human exposure to airborne PM, although ingestion, dermal contact, and ocular exposure may also contribute to the overall exposure burden (Thompson, 2018; WHO, 2005). Fine and ultrafine particles can penetrate deeply into the respiratory tract and enter the systemic circulation, promoting oxidative stress, inflammation, vascular dysfunction, and immune dysregulation (Costa et al., 2019; Kang et al., 2021; Traboulsi et al., 2017). Beyond these systemic effects, accumulating evidence indicates that PM can also affect the central nervous system (CNS), with neuroinflammation emerging as a major biological pathway linking AP to brain dysfunction. Accordingly, PM exposure has been associated not only with neurodegenerative diseases in adulthood but also with altered neurodevelopmental trajectories following early-life exposure (Block and Calderón-Garcidueñas, 2009; Costa et al., 2020, 2019).

The developing brain is particularly vulnerable to environmental insults because critical neurodevelopmental processes, including neurogenesis, synaptogenesis, gliogenesis, myelination, and circuit refinement, occur within tightly regulated temporal windows (Costa et al., 2004; Deidda et al., 2021; Rodier, 1994). Exposure to environmental toxicants during these sensitive periods may induce persistent alterations in neuronal connectivity, neurotransmission, neuroimmune signaling, and behavioral function. In line with this concept, epidemiological and preclinical studies have linked prenatal and early-life AP exposure to adverse neurodevelopmental outcomes, including autism spectrum disorder (ASD)-like behaviors, delayed developmental milestones, and cognitive and social alterations (Rodulfo-Cárdenas et al., 2023; Ruiz-Sobremazas et al., 2023). At the molecular level, these outcomes have been associated with disruptions in neuroinflammatory, oxidative-stress, synaptic, immune-related, neurotransmitter, myelin-related and stress-response pathways (Pan et al., 2020; Rodulfo-Cárdenas et al., 2023; Ruiz-Sobremazas et al., 2023; Thomson, 2019; Zhang et al., 2024).

Despite growing evidence linking PM exposure to adverse neurodevelopmental outcomes, individual responses to environmental pollutants are highly heterogeneous. Genetic background is increasingly recognized as an important determinant of susceptibility to environmental toxicants (Kleeberger and Ohtsuka, 2005; Thier et al., 2002). Within this framework, apolipoprotein E (APOE) is the major apolipoprotein in the CNS and plays a central role in brain lipid transport and homeostasis. Among the three major human *APOE* alleles (ε2, ε3, and ε4), *APOE* ε3 is the most prevalent allele in the general population, whereas *APOE* ε4 is the strongest genetic risk factor for Alzheimer's disease (AD) (Liu et al., 2013a; Serrano-Pozo et al., 2021). Importantly, *APOE* ε4 has also been associated with altered neuroimmune responses, increased oxidative stress, impaired synaptic plasticity, mitochondrial dysfunction, and reduced resilience to environmental stressors (Calderón-Garcidueñas et al., 2023; Dose et al., 2016; Jofre-Monseny et al., 2008). Beyond its role in neurodegeneration, APOE also contributes to key biological processes involved in early brain maturation, including synapse formation and plasticity, regulation of neuronal and glial development, repair mechanisms, and myelin formation (Dean et al., 2014; Liu et al., 2013b).

Consistent with this developmental role, emerging evidence suggests that *APOE* genotype may modulate the neurodevelopmental consequences of AP exposure. Studies in children and young individuals exposed to traffic-related AP and PM indicate that *APOE* ε4 carriers may exhibit poorer cognitive performance, increased behavioral and attentional problems, neuroinflammatory and cerebrovascular alterations, and changes in brain structure compared with non-carriers or less susceptible genetic profiles (Alemany et al., 2018; Calderón-Garcidueñas et al., 2023; Calderón-Garcidueñas and De La Monte, 2017). These findings support the idea that *APOE* genotype may influence biological vulnerability to environmental pollutants early in life, long before the emergence of overt neurodegenerative phenotypes. However, experimental evidence addressing how human APOE isoforms shape the long-term consequences of developmental PM exposure remains limited.

Biological sex may further shape vulnerability to environmental toxicants and APOE-related effects. Sex-dependent responses to AP have been reported across the life course, suggesting that males and females may differ in their biological sensitivity to airborne pollutants (Clougherty, 2009). This is particularly relevant during early development, when male and female brains follow partially distinct maturational trajectories shaped by hormonal, genetic, and immune-related mechanisms. For instance, sex differences in the activation state of innate immune cells during brain development may contribute to differential vulnerability to early environmental challenges, with males often proposed to be more susceptible to neurodevelopmental disruption (Lenz and McCarthy, 2014). In line with this, preliminary human and animal evidence suggests that males may show greater susceptibility to the neurotoxic effects of AP than females (Suades-González et al., 2015). At the same time, APOE-related effects are also sex-dependent, as *APOE* ε4 allele confers a greater risk for AD in women than in men (Altmann et al., 2014; Riedel et al., 2016). Thus, sex may interact with both environmental exposure and *APOE* genotype to influence neurodevelopmental vulnerability, yet this three-way relationship remains poorly characterized.

Previous research from our laboratory has demonstrated that early postnatal PM exposure disrupts normal weight gain in females and delays neuromotor development. In addition, PM effects were partially modulated by *APOE* genotype: apoE3 mice showed accelerated eye and vaginal opening, whereas apoE4 mice exhibited more pronounced biochemical alterations involving inhibitory/excitatory balance, serotonergic homeostasis, and Reelin-mediated synaptic plasticity (Rodulfo-Cárdenas et al., 2026). These findings suggest that early PM exposure can induce genotype- and sex-dependent developmental effects, but whether these early alterations translate into persistent behavioral and molecular changes later in life remains unknown. Building on this work, the present study investigated whether early postnatal PM inhalation, during a developmental window that overlaps, in terms of key brain-maturation processes, with late gestation and the early neonatal period in humans (Semple et al., 2013; Zeiss, 2021), leaves a persistent behavioral and molecular signature in young adult humanized apoE3 and apoE4 transgenic mice. To this end, we assessed behavioral domains related to motor coordination, emotionality, sociability, motivation, and spatial learning, together with gene-expression profiles in the hippocampus (HPC) and striatum (STR), two brain regions critically involved in cognitive, affective, motivational, and motor-related functions. This approach allowed us to determine whether *APOE* genotype and biological sex act as key modulators of long-term susceptibility to developmental PM toxicity.

2. Materials and methods

2.1. Experimental animals

Humanized apoE3 (JAX Stock No. 029018) and apoE4 (JAX Stock No. 027894) targeted replacement (TR) mouse lines were obtained from The Jackson Laboratory (Bar Harbor, ME, USA). Both lines were maintained on a C57BL/6 background and had been generated by substituting the murine ApoE locus with the human *APOE* ε3 or ε4 alleles (Foley et al., 2022). The apoE3 colony was established in-house through initial heterozygote × wild-type matings. Heterozygous F1 offspring were identified by genotyping and subsequently intercrossed to generate homozygous apoE3 animals, whereas apoE4 mice were purchased as homozygous animals. Homozygous animals of each genotype were subsequently bred in our facility to generate the experimental litters, and the genotype of all offspring was confirmed before allocation. Breeder females had produced one previous litter before the experimental mating. Male–female pairs of the same genotype (1:1)

were co-housed for 2 days to permit mating. Females were weighed on gestational days 0, 10, and 15 to monitor pregnancy progression. On day 15 of presumed gestation, pregnant females were singly housed, and the day of parturition was designated postnatal day (PND) 0. Litters were standardized to six pups per dam and randomly allocated to control (CNT) or exposure (PM) groups. For post-weaning behavioral and molecular analyses, one male and one female per litter were selected to minimize litter-related effects and avoid pseudoreplication. After weaning at PND28, offspring were housed in plastic cages (2–4 mice per cage), grouped by genotype and sex, with environmental enrichment consisting of nesting material and wooden structures. Animals were maintained under controlled conditions (temperature, 22 ± 2 °C; relative humidity, 50 ± 10%) on a 12-h light/dark cycle (lights on 08:00–20:00 h). Standard chow diet (SAFE® A04 diet; Panlab, Barcelona, Spain) and tap water were provided *ad libitum*. All procedures were approved by the Animal Care and Use Committee of the Rovira i Virgili University (Tarragona, Spain) and by the Government of Catalonia (approval no. 12131). Experiments were conducted in accordance with the ARRIVE guidelines (Percie du Sert et al., 2020), the EU Directive 2010/63/EU on the protection of animals used for scientific purposes, and the Spanish Royal Decree 53/2013.

2.2. Particulate matter exposure and experimental design

Mice were exposed daily to either 0.9% saline (CNT) or a suspension of Fine Atmospheric Particulate Matter (PM; mean particle diameter <10 μm; Standard Reference Material 2787, NIST), a commercially available reference material originally collected from an air intake filtration system and developed as a standardized atmospheric PM sample. Detailed information regarding its organic and inorganic composition, certified and non-certified constituent values, and particle-size characteristics is provided in the NIST Certificate of Analysis (Gonzalez and Choquette, 2021). PM suspensions were prepared in 0.9% saline and sonicated for 10 min immediately before each exposure session to ensure uniform dispersion. Exposures were performed using a compartmentalized whole-body inhalation chamber connected to a nebulization system (Buxco Mass Dosing Chamber, DSI™/Harvard Bioscience). An inhalation-based paradigm was selected because inhalation represents the primary route of human exposure to airborne PM (Thompson, 2018), thereby providing greater route-of-exposure relevance than direct administration procedures.

The nominal target dose used for the design of the study was selected based on ambient PM concentrations previously reported in Tarragona province (Spain). Environmental monitoring in this area has generally reported $PM_{2.5}$ concentrations of approximately 15–25 μg/m^3 and PM_{10} concentrations of approximately 25–40 μg/m^3, depending on season and climatic conditions (Sánchez-Soberón et al., 2019). Considering an adult human body weight of 70 kg and an inhaled air volume of approximately 20 m^3/day, the corresponding daily inhaled PM burden is estimated at approximately 19–20 μg/kg/day. A tenfold factor was subsequently applied to account conservatively for interspecies variability (EPA, 2002), resulting in the nominal experimental target of 200 μg/kg/day. In a global context, the reported local $PM_{2.5}$ concentrations are below the estimated worldwide urban average for 2019 (35 μg/m^3) and below those observed in the most polluted urban regions (Southerland et al., 2022). Nevertheless, they exceed the WHO annual AQG values of 5 μg/m^3 for $PM_{2.5}$ and 15 μg/m^3 for PM_{10} (WHO, 2021), supporting their environmental and public-health relevance.

The exposure regimen was therefore conceived as a temporally compressed, high-exposure experimental scenario intended to approximate within a 1-h daily session a PM burden that, in humans, would accumulate over a substantially longer period of continuous ambient exposure. The 1-h session was selected to limit the time that dams and litters remained in the exposure chamber and thereby minimize procedure-related stress. The resulting target dose was used as a nominal value for configuring the experimental exposure rather than as a direct measurement of the dose inhaled by the animals. Chamber loading was calculated assuming a mean adult-mouse body weight of 30 g and an estimated daily respiratory volume of 0.038 m^3 (Office of Environmental Health Hazard Assessment, 2005), corresponding to approximately 0.001583 m^3 during a 1-h exposure. Under these assumptions, a nominal dose of 200 μg/kg corresponded to 6 μg per adult-mouse equivalent. Considering an aggregate respiratory-volume approximation of eight adult-mouse equivalents per chamber, the target airborne concentration was calculated as approximately 3789 μg/m^3. Based on the chamber volume of 0.014 m^3, this concentration corresponded to a total nominal PM load of approximately 53.05 μg.

The calculated concentration of 3789 μg/m^3 represents a theoretical maximum chamber concentration, assuming complete aerosolization and homogeneous distribution, maintenance of a constant airborne concentration throughout the 1-h exposure period, and no particle losses. The PM load was suspended in 3 mL of 0.9% saline and nebulized over approximately 30 min. Animals remained in the chamber for an additional 30 min after nebulization, resulting in a total exposure-session duration of 1 h. Because aerosol concentration was not monitored continuously and the chamber was not airtight, the calculation did not account for ventilation, leakage, sedimentation, deposition on chamber surfaces, or temporal changes in aerosol concentration. Therefore, neither the theoretical chamber concentration nor the nominal target dose should be interpreted as the actual inhaled or pulmonary-deposited dose. A step-by-step summary of the assumptions, input parameters, and calculations used to derive the nominal target dose and theoretical maximum chamber concentration is provided in Supplementary Table S1. Further technical details of the chamber configuration and aerosol generation are provided in our previous publication (Rodulfo-Cárdenas et al., 2026).

To habituate females to the exposure procedure, animals intended for breeding were placed in the exposure chamber for 5 consecutive days during the week preceding mating. Exposures were conducted in a room separate from the housing facility for 1 h per day from PND4 to PND14. During each exposure session, dams remained together with their litters to minimize stress and preserve animal welfare conditions. Behavioral assessments covering motor coordination and learning, locomotor activity, anxiety-like behavior, social behavior, anhedonia-like behavior, and spatial learning and memory were performed in young adult animals between PND50 and PND96. On the day after completion of the last behavioral assessment, the animals were euthanized and biological samples were collected for subsequent analyses. The overall experimental design, including the exposure window, behavioral assessment sequence, and sacrifice, is summarized in Fig. 1.

2.3. Motor function assessment

Motor coordination and learning were assessed using the Rotarod test (Shiotsuki et al., 2010). The apparatus consisted of a rotating cylinder elevated above a padded surface, allowing evaluation of the animal's ability to maintain balance on the rod. The test was conducted over two consecutive days. On the first day, animals performed two acquisition trials at a constant speed of 16 rpm, separated by a 30-min inter-trial interval. In each trial, animals were required to remain on the rotating rod for a maximum of 120 s; when an animal fell, it was placed back on the cylinder, and the trial continued until the total trial duration was completed. On the second day, animals performed a final acquisition trial, followed 2 h later by the test session. The test session followed an accelerating protocol, starting at 16 rpm and ending when the animal fell or when the maximum duration of 120 s was reached. During acquisition, latency to first fall, total number of falls, and number of flips were recorded. During the test session, latency to fall and maximum speed reached were analyzed.

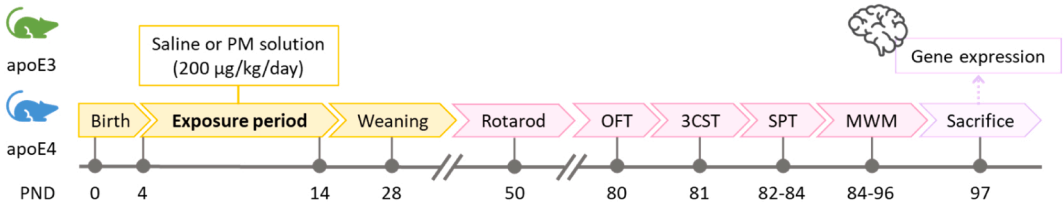


Fig. 1. Experimental timeline. Schematic overview of the early postnatal exposure period, behavioral assessment sequence, and sacrifice in humanized apoE3 and apoE4 mice. Mice were exposed daily to saline or PM solution from PND4 to PND14. Motor function was assessed at PND50, followed by the behavioral test battery from approximately PND80 to PND96. Animals were sacrificed at PND97 for subsequent gene-expression analyses. Abbreviations: Morris Water Maze (MWM), Open Field test (OFT), Particulate matter (PM), Postnatal day (PND), Sucrose Preference test (SPT), Three-Chamber Social test (3CST).

2.4. Behavioral tests

Behavioral tests were performed during the light phase (08:30–14:00) and conducted in a dedicated experimental room maintained at 22 ± 2 °C under white overhead light. Animals were transferred to the testing room 10 min prior to the start of testing to allow acclimation. All behavioral tests were recorded and tracked using a C920 Pro HD webcam (Logitech, Switzerland) connected to EthoVision XT 17 software (Noldus Information Technologies, Wageningen, The Netherlands). In the Open Field Test (OFT) and the Three-Chamber Social Test (3CST), boxes were cleaned with 70% ethanol between trials to avoid olfactory cues.

The behavioral battery was performed in a fixed order: OFT, 3CST, sucrose preference test (SPT), and Morris water maze (MWM). This sequence was selected to progress from tests involving relatively low stress and limited learning demands to more demanding or potentially stressful procedures, thereby minimizing carryover effects on subsequent outcomes. The MWM was performed last because repeated swimming, escape learning, and the associated handling could induce stress or learning-related effects capable of influencing performance in the other tests. Although carryover effects cannot be completely excluded in a repeated-testing design, all animals underwent the same sequence, thereby standardizing testing history across experimental groups.

2.4.1. Open field test

Locomotor activity and anxiety-like behavior were evaluated using the OFT (Peris-Sampedro et al., 2020). The OF apparatus consisted of an open-top square wooden box (60 × 60 cm base, 50 cm wall height). The field was virtually divided into two zones: the periphery, defined as the 15-cm area adjacent to the walls, and the center. Each subject was placed in the center of the field at the beginning of the trial and allowed to explore freely for 30 min. Locomotor activity was quantified as the total distance traveled and mean velocity, and habituation to the novel environment was assessed as the progressive change in locomotor activity across consecutive 5-min intervals. Anxiety-like behavior was inferred from center-related measures, including total distance traveled, mean velocity, time spent in the center, frequency of center entries, and the ratio of distance traveled in the center to total distance. Trials in which the animal was not detected for more than 10% of the recording time were further inspected to assess whether the tracking loss occurred in the peripheral zone. In such cases (n = 7), total distance traveled, mean velocity, and distance-based ratios were excluded from the analysis, while center-related parameters were still included. In addition, one apoE3 CNT male was excluded from the OFT analysis as an outlier based on total distance traveled.

2.4.2. Three-chamber social test

Sociability and social novelty preference were assessed using the 3CST (Basaure et al., 2019). The apparatus consisted of an open-top Plexiglas box (60 × 30 × 30 cm) divided into three interconnected chambers (20 × 30 × 30 cm) by two transparent walls with doorways, allowing the mouse to move freely between compartments. Both lateral chambers contained an empty wire cup (7 × 7 cm) positioned in the lower corner. The procedure comprised three phases. In the habituation phase, the mouse was placed in the central chamber and allowed to explore freely for 10 min. In the sociability phase, one unfamiliar conspecific of the same sex and age was placed under one wire cup (social chamber), while an inanimate object (red plastic frog, 2.5 × 2.5 cm) was placed under the other wire cup (non-social chamber). In the social novelty phase, the inanimate object was replaced with a novel unfamiliar mouse of the same sex and age (novelty chamber), while the now-familiar mouse from the previous phase remained under its original wire cup. In the latter two phases, the animal was allowed 6 min of free exploration. During the habituation phase, general locomotor measures (total distance traveled and mean velocity) were assessed, and the time spent in each chamber was analyzed to detect any baseline side preference. During the sociability and social novelty phases, general locomotor measures (distance traveled and velocity) were also assessed, together with the time spent in the social or novel chamber. Additionally, a social preference ratio was calculated as: (time in social chamber − time in non-social chamber)/(time in social chamber + time in non-social chamber). Across trials, the location of the social stimulus was counterbalanced between the left and right chambers to minimize potential side bias. Trials in which the animal was not detected for more than 10% of the recording time were visually inspected to identify the location of tracking loss and determine data inclusion. During the social novelty phase, three animals exceeded this threshold; however, video inspection confirmed that tracking loss occurred while the animals remained in the novel social chamber, and therefore these trials were also retained. In addition, one apoE3 PM male and two apoE4 PM females were excluded from the social novelty analysis because of tracking failures.

2.4.3. Sucrose preference test

Anhedonia was evaluated using the SPT based on a two-bottle choice paradigm (Liu et al., 2018). Two days before testing, animals were familiarized with the presence of two bottles in their home cages (both bottles filled with water). The SPT was conducted over three consecutive days. During each daily 4-h testing session, animals were temporarily transferred to individual cages to enable accurate measurement of fluid intake for each mouse and were given access to two bottles, one containing water and the other containing a 4% (w/v) sucrose solution. To minimize side bias, bottle positions were switched 2 h after the onset of each session. Food remained available *ad libitum* throughout testing. Bottles were weighed immediately before and after each session to quantify fluid intake, and sucrose preference (%) was calculated as: (sucrose intake / total fluid intake) × 100.

2.4.4. Morris water maze test

Spatial learning and memory were assessed using the MWM (Morris, 1984). The apparatus consisted of a circular pool (diameter, 100 cm; height, 60 cm) virtually divided into four quadrants. A circular escape platform (diameter, 10 cm) was positioned at the center of the target quadrant (TQ), submerged 1 cm below the water surface. The pool was filled with a water-latex mixture to conceal the platform. Black

geometric figures affixed to the surrounding walls served as distal visual cues. Four starting points and four positions for an inner rotating wall were predefined and varied across trials to minimize intra-maze cues and promote allocentric navigation (Reverte et al., 2012).

Animals were habituated to the aquatic environment for 45 s without the platform. Three days later, the acquisition phase began and comprised 20 trials (4 trials/day for five consecutive days; 30-min inter-trial interval). In each trial, animals had 90 s to locate the hidden platform; upon locating it, they remained on the platform for 30 s. If an animal failed to locate the platform, the experimenter guided it to the platform, where it remained for 30 s. After each trial, animals were dried in a clean cage under infrared light. During acquisition, distance traveled, swim velocity, and latency to reach the platform were analyzed as indices of learning. Short- and long-term memory were assessed in probe trials (platform removed) conducted 4 h after the last acquisition day and again at 72 h later. In each probe trial, mice were released into the pool and allowed to swim freely for 60 s. Total distance, mean velocity, and time spent in the TQ were analyzed. Following the 72-h probe, the reversal phase commenced. The platform was relocated to the quadrant opposite the original TQ, and animals again had 90 s per trial. This phase included 8 trials (4 trials/day over two consecutive days), and the same outcome measures as in acquisition were analyzed. Four hours after the start of the second reversal day, a final probe trial was performed to assess memory for the new platform location and cognitive flexibility. On the last day, the visual phase was conducted by attaching a salient visual cue to the platform to exclude visual deficits; animals had 90 s per trial. This phase comprised 4 trials conducted on a single day, and the same acquisition measures were analyzed. Body weight was monitored on days 1, 5, and 8 of the MWM protocol as a welfare control measure.

2.5. Sacrifice and sampling

Animals were euthanized on the day following completion of the behavioral tests. Before euthanasia, they were subjected to a 4-h fasting period. Anesthesia was induced by inhalation of isoflurane (Vetflurane, 1000 mg/g, Virbac Spain, S.A.) using a low-flow anesthesia system (SomnoSuite®, Kent Scientific Corporation, USA). After confirming loss of reflexes and adequate anesthetic depth, cardiac exsanguination was performed to obtain plasma samples using EDTA tubes (K2E Tubes; BD Microtainer®, USA). Death was confirmed by cervical dislocation, and the following brain regions were rapidly dissected: olfactory bulb, frontal cortex, STR, HPC, hypothalamus, and brainstem together with cerebellum. Samples were immediately snap-frozen on dry ice and stored at −80 °C until analysis.

2.6. Gene expression analysis

The HPC and STR were selected for gene-expression analyses because of their complementary involvement in the behavioral domains assessed. The HPC plays a central role in spatial learning and memory, including acquisition, retention, and reversal performance in the MWM (Dong et al., 2013; Morris et al., 1982; Vorhees and Williams, 2014), and also contributes to contextual processing (Anagnostaras et al., 2001), anxiety-related behavior (Kjelstrup et al., 2002), and social recognition (Tanimizu et al., 2017). The STR is critically involved in locomotor and motor function, action selection, procedural learning, motivation, reward processing, and social behavior (Báez-Mendoza and Schultz, 2013; Graybiel and Grafton, 2015; Kreitzer and Malenka, 2008; Liang et al., 2022; Liljeholm and O'Doherty, 2012), making it relevant to outcomes assessed in the Rotarod, OFT, 3CST, SPT, and MWM. Moreover, the HPC and STR are thought to cooperate closely during navigation rather than functioning as parallel and independent systems, further supporting the relevance of examining both regions in relation to MWM performance (Miyoshi et al., 2012). Together, these regions allowed us to investigate molecular pathways associated with cognitive, emotional, motor, social, and reward-related outcomes.

Total RNA was extracted using the NZY DNA/RNA/Protein Isolation Kit (Ref. MB45901; NZYtech, Lisbon, Portugal). Samples were processed under coded identifiers, and genotype, sex, and treatment groups were distributed across extraction batches to reduce systematic batch-related variation. RNA concentration and purity were determined using a Nanodrop 2000 spectrophotometer (Thermo Fisher Scientific, Waltham, MA, USA). Complementary DNA (cDNA) was synthesized from RNA samples using the Maxima First Strand cDNA Synthesis Kit for RT-qPCR (Ref. K1642; ThermoFisher Scientific, Waltham, MA, USA). For each sample, standardized amounts of 718.2 ng of total hippocampal RNA and 273.7 ng of total striatal RNA were reverse-transcribed, resulting in final cDNA concentrations of 11.97 ng/μL and 4.56 ng/μL, respectively.

Real-time quantitative polymerase chain reaction (RT-qPCR) was used to assess gene expression, employing the Maxima SYBR Green/ROX qPCR Master Mix (2X) Kit (Ref. K0222; Thermo Fisher Scientific, Waltham, MA, USA). The target genes analyzed in each brain region and the corresponding primer sequences are provided in Supplementary Table S2. Primer specificity was evaluated *in silico* using NCBI Primer-BLAST, and amplification efficiency was determined for each primer pair. Reactions were run in triplicate, and quantification cycle (Cq) values were acquired with a QuantStudio™ 5 Real-Time PCR System (Thermo Fisher Scientific, Waltham, MA, USA). When the standard deviation of triplicate Cq values exceeded 0.3 (Applied Biosystems, 2008), individual replicates were inspected to determine whether a technical outlier could be identified and excluded. If no clear outlier was detected, the corresponding sample was removed from further analysis.

To identify the most suitable reference genes for normalization, five candidate housekeeping genes (*Gapdh*, *Hprt1*, *Rpl13a*, *Sdha* and *Tbp*) (Yin et al., 2010) were evaluated for expression stability independently in each tissue using RefFinder, a web-based tool that integrates geNorm, NormFinder, BestKeeper, and the comparative ΔCq method to rank candidate reference genes (Xie et al., 2012). The potential benefit of including a third reference gene was also assessed. Based on the overall results, *Gapdh* and *Hprt1* were identified as the two most stable reference genes and were therefore selected for normalization in both tissues. Relative quantity (RQ) values were calculated for each sample using the formula $RQ=E^{-Cq}$, where E represents the amplification efficiency of the corresponding primer pair, following the efficiency-corrected approach described by Pfaffl (2001). A normalization factor (NF) was then obtained as the geometric mean of the RQ values of the two selected reference genes, according to the method proposed by Vandesompele et al. (2002). Normalized relative quantity (NRQ) was subsequently calculated for each target gene by dividing its RQ value by the corresponding NF. Fold change values were then obtained by normalizing each NRQ value to the geometric mean NRQ of the male apoE3 control group, which was used as the reference group.

2.7. Statistical analysis

Statistical analyses were performed using IBM SPSS Statistics version 31.0 software (IBM Corp., NY, USA). Potential outliers were identified using Grubbs' test ($\alpha=0.05$). Data are presented as mean ± standard error of the mean (SEM). Statistical significance was set at $p \leq 0.05$, while values between $p > 0.05$ and $p < 0.10$ were considered trends. Full statistical outputs for all analyses are provided in the Supplementary Material (Table S3-S18).

Genotype, sex, and treatment were included as the main experimental factors in the statistical models. Depending on the outcome variable and experimental design, data were analyzed using univariate analysis of variance (ANOVA) or repeated-measures ANOVA (RM-ANOVA). Univariate ANOVA was used for single-time-point outcomes, including body weight, Rotarod test performance, and selected behavioral and molecular endpoints. RM-ANOVA was used for repeated measures across time, trials, days, or chambers, including OFT, 3CST, SPT, and MWM. For RM-ANOVA, multivariate statistics were considered, with Pillai's trace used for within-subject effects. When significant

interaction effects were detected, simple-effects analyses were performed using estimated marginal means with Bonferroni adjustment for multiple comparisons. One-sample t-tests were used for the 3CST, SPT, and MWM probe trials to assess whether preference or memory-related measures differed from their corresponding theoretical chance levels.

For Rotarod acquisition, distributional properties were specifically inspected using descriptive statistics, skewness, kurtosis, normality tests, frequency distributions, and visual inspection. Latency to first fall showed positive skewness, particularly during the first acquisition trial; therefore, values were natural log-transformed and analyzed using a repeated-measures general linear model. The number of falls was treated as count data. Because descriptive inspection showed positive skewness, overdispersion, and an increasing proportion of zero values across acquisition trials, falls were analyzed using a generalized linear mixed model with a negative binomial distribution and log-link function. Trial, genotype, sex, and treatment were included as fixed factors, together with their interactions, and animal ID was included as a random intercept to account for repeated observations within animals. During the Rotarod test phase, latency to fall and maximum speed reached were analyzed using separate univariate ANOVA.

Potential associations between individual body weight and selected behavioral outcomes were assessed using partial correlations controlling for genotype, sex, and treatment. These included Rotarod test-phase latency, OFT total distance, and mean MWM acquisition velocity and latency. When a significant association was detected, a sensitivity analysis was performed by adding body weight as a covariate to the original factorial model after verifying homogeneity of regression slopes.

For the RT-qPCR analyses, each gene and brain region was analyzed separately according to the factorial experimental design. Bonferroni adjustment was applied to estimated marginal-mean comparisons performed following significant interaction effects. No additional correction was applied across the complete set of genes, model effects, and brain regions because the candidate-gene analyses were intended as exploratory and hypothesis-generating, with the aim of identifying molecular pathways and potential targets for subsequent validation. Accordingly, RT-qPCR p-values are reported as nominal values, and the molecular findings should not be interpreted as confirmatory evidence.

3. Results

3.1. PM exposure increases post-weaning weight gain in apoE3 females

Because body weight is inherently sex-dependent from early development, body-weight analyses were stratified by sex. To avoid litter-related pseudoreplication, the litter was used as the experimental unit, and body-weight values were expressed as the mean weight of pups within each litter. At PND28 (Fig. 2A), corresponding to weaning, males showed a significant Genotype effect, with apoE4 males weighing more than apoE3 males [$F_{1,47}$= 4.164, p = 0.047, η_p^2= 0.081], whereas PM-exposed females tended to weigh less than controls [$F_{1,48}$= 3.458, p = 0.069]. No significant effects were detected at PND50 or PND70 in either sex.

Body-weight gain from PND28 to PND70 (Fig. 2B) was then analyzed to evaluate post-weaning growth. In males, apoE3 mice showed significantly greater weight gain than apoE4 mice [$F_{1,46}$= 4.268, p = 0.044, η_p^2= 0.085]. In females, weight gain was significantly affected by Genotype [$F_{1,47}$= 8.131, p = 0.006, η_p^2= 0.147] and Treatment [$F_{1,47}$= 11.255, p = 0.002, η_p^2= 0.193], with a significant Genotype × Treatment interaction [$F_{1,47}$= 5.047, p = 0.029, η_p^2= 0.097]. Simple-effects analyses showed that apoE3 PM-exposed females gained more weight than apoE4 PM-exposed females [$F_{1,47}$= 12.772, p < 0.001, η_p^2= 0.214], and PM exposure increased weight gain specifically in apoE3 females compared with their controls [$F_{1,47}$= 14.826, p < 0.001, η_p^2= 0.240].

3.2. Motor coordination and learning are modulated by genotype and sex

During Rotarod acquisition, latency to the first fall (Fig. 3A) increased significantly across trials [$F_{2,75}$ = 326.871, p < 0.001, η_p^2= 0.897], reflecting progressive improvement in motor performance. Moreover, the temporal dynamics of motor learning showed a significant Trial × Genotype × Sex × Treatment interaction [$F_{2,75}$ = 4.300, p = 0.017, η_p^2= 0.103], indicating that the evolution of initial motor performance depended on the combined influence of genotype, sex, and PM exposure. Follow-up comparisons based on estimated marginal means showed that, in apoE4 males, PM-exposed animals performed better than controls, as reflected by higher latency to fall at Trial 1 [$F_{1,76}$

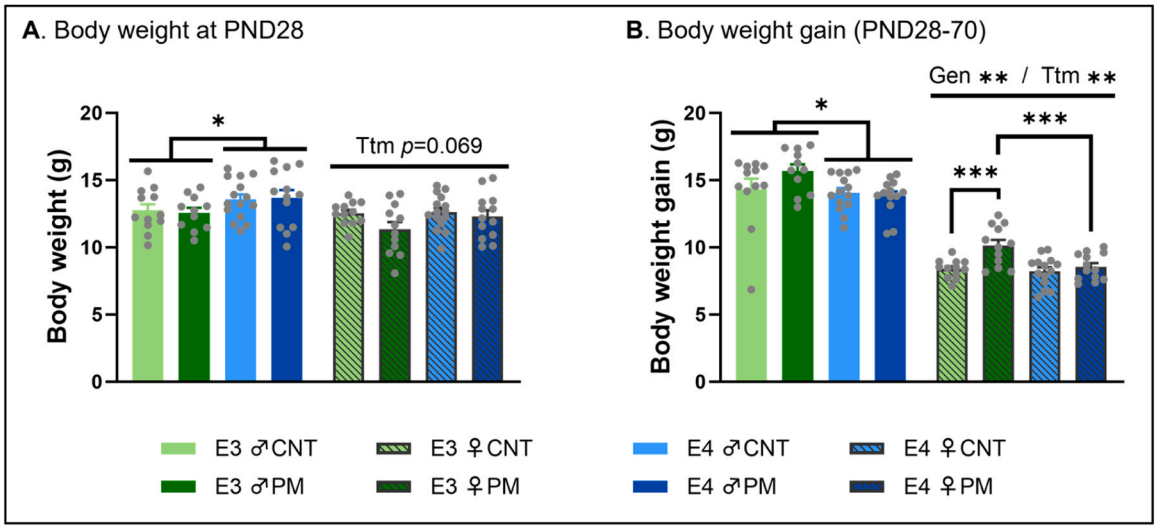


Fig. 2. Body weight analysis. At PND28, apoE4 males exhibited higher body weight than apoE3 males, whereas PM-exposed females showed a trend toward lower body weight compared with controls (A). Regarding body weight gain from PND28 to PND70, apoE3 males gained more weight than apoE4 males, while apoE3 PM-exposed females displayed greater weight gain than both apoE3 control females and apoE4 PM-exposed females (B). Data are presented as mean ± SEM. The litter was used as the statistical unit for body-weight analyses: apoE3 male CNT (n = 12), apoE3 male PM (n = 11), apoE3 female CNT (n = 12), apoE3 female PM (n = 12), apoE4 male CNT (n = 15), apoE4 male PM (n = 13), apoE4 female CNT (n = 15), apoE4 female PM (n = 13). *p ≤ 0.05, **p < 0.01, ***p < 0.001. Abbreviations: ApoE3 mice (E3), ApoE4 mice (E4), Control (CNT), Genotype (Gen), Particulate matter (PM), Postnatal day (PND), Treatment (Ttm).

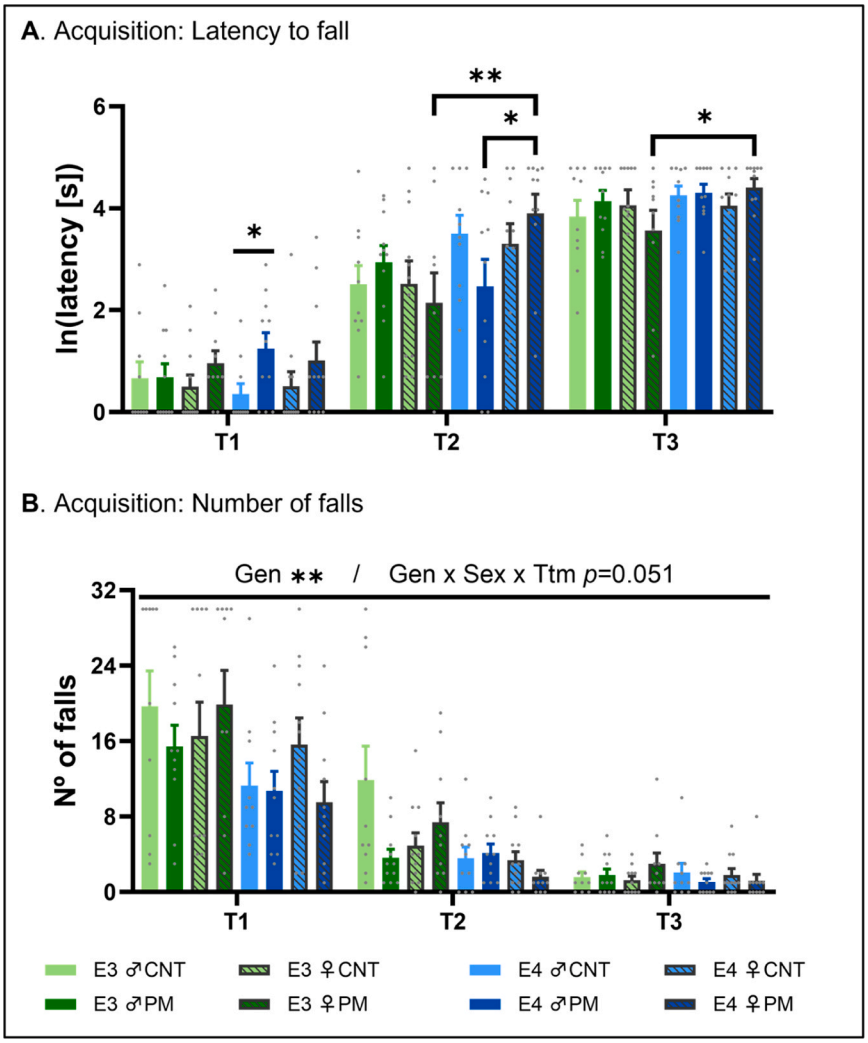


Fig. 3. Rotarod Test. Latency to first fall increased across trials, indicating progressive improvement in motor performance, with genotype-, sex-, and treatment-dependent differences during acquisition (A). Falls decreased across trials, consistent with motor learning/adaptation, and apoE3 mice showed a higher number of falls than apoE4 mice (B). Data are presented as mean ± SEM. ApoE3 male CNT (n = 10), apoE3 male PM (n = 11), apoE3 female CNT (n = 11), apoE3 female PM (n = 10), apoE4 male CNT (n = 10), apoE4 male PM (n = 11), apoE4 female CNT (n = 11), apoE4 female PM (n = 11). *p ≤ 0.05, **p < 0.01. Abbreviations: ApoE3 mice (E3), ApoE4 mice (E4), Control (CNT), Genotype (Gen), Particulate matter (PM), Treatment (Ttm), Trial (T).

= 4.804, $p = 0.031$, $\eta_p^2 = 0.059$]. Among PM-exposed females, apoE3 mice showed lower latency than apoE4 mice at Trial 2 [$F_{1,76} = 7.933$, $p = 0.006$, $\eta_p^2 = 0.095$] and Trial 3 [$F_{1,76} = 6.516$, $p = 0.013$, $\eta_p^2 = 0.079$]. In addition, within PM-exposed apoE4 mice, males showed lower latency than females at Trial 2 [$F_{1,76} = 5.861$, $p = 0.018$, $\eta_p^2 = 0.072$]. The number of falls (Fig. 3B) progressively decreased across acquisition trials [$F_{2,231} = 122.951$, $p < 0.001$], consistent with motor learning/adaptation over repeated exposure to the task. A general Genotype-dependent effect was also observed [$F_{1,231} = 7.328$, $p = 0.007$], with apoE3 mice showing a higher number of falls than apoE4 mice, together with a trend toward Genotype × Sex × Treatment interaction [$F_{1,231} = 3.860$, $p = 0.051$]. No treatment-related interactions were detected for this parameter, suggesting that PM exposure did not produce a consistent alteration in overall acquisition performance. No significant differences were observed in the analyzed parameters during the test phase. Body weight at PND50 was not significantly associated with test-phase latency to fall after controlling for genotype, sex, and treatment (partial r = −0.059, $p = 0.601$).

3.3. *Genotype and sex shape locomotor activity and anxiety-like behavior in the Open field test*

In the OFT, total distance traveled (Fig. 4A) and mean velocity (Fig. 4B) were used as measures of general locomotor activity. For both parameters, significant effects of Genotype (distance:[$F_{1,68} = 4.771$, $p = 0.032$, $\eta_p^2 = 0.066$], velocity: [$F_{1,68} = 5.544$, $p = 0.021$, $\eta_p^2 = 0.075$]) and Sex (distance:[$F_{1,68} = 16.100$, $p < 0.001$, $\eta_p^2 = 0.191$], velocity: [$F_{1,68} = 10.265$, $p = 0.002$, $\eta_p^2 = 0.131$]) were observed. Overall, apoE3 mice showed higher locomotor activity than apoE4 mice, as reflected by greater distance traveled and higher mean velocity; similarly, males displayed higher locomotor activity than females. Distance traveled was also analyzed in 10-min intervals to assess habituation to the novel environment. This analysis revealed significant effects of Time [$F_{2,67} = 30.483$, $p < 0.001$, $\eta_p^2 = 0.476$], consistent with habituation to the novel environment, Time × Sex [$F_{2,67} = 7.805$, $p < 0.001$, $\eta_p^2 = 0.189$] and a Time × Sex × Treatment interaction [$F_{2,67} = 3.599$, $p = 0.033$, $\eta_p^2 = 0.097$] (Fig. 4C). Follow-up simple effects analyses based on estimated marginal means with Bonferroni adjustment showed that males traveled a greater distance than females during the first 20 min, both in the 0–10 min interval [$F_{1,68} = 15.470$, $p < 0.001$, $\eta_p^2 = 0.185$] and in the 10–20 min interval [$F_{1,68} = 20.895$, $p < 0.001$, $\eta_p^2 = 0.235$]. When

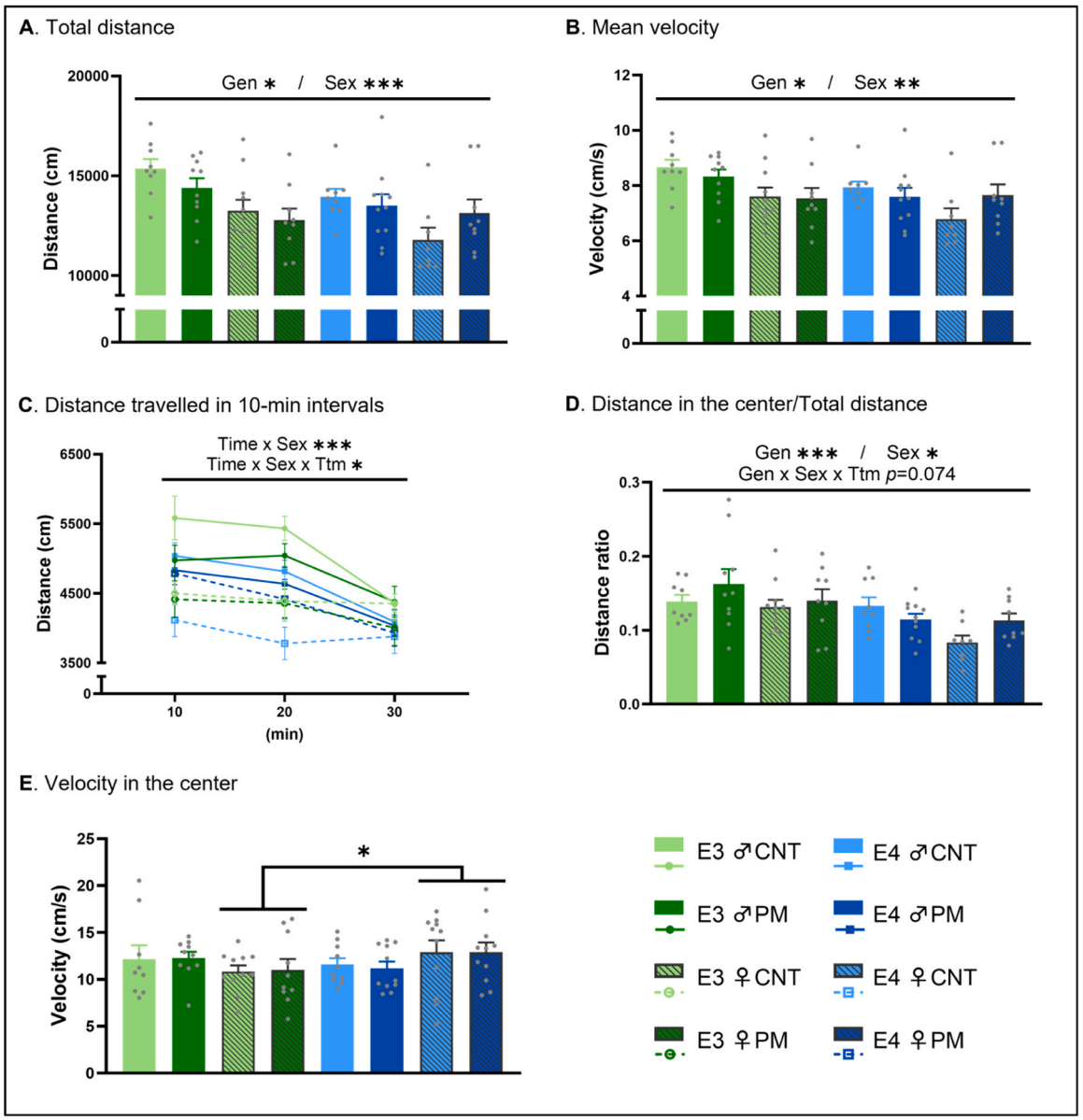


Fig. 4. Open Field Test. Total distance travelled (A) and mean velocity (B) indicated higher locomotor activity in apoE3 than in apoE4 mice, and in males compared with females. Distance travelled across consecutive 10-min intervals progressively decreased over time, with sex- and treatment-dependent modulation of this habituation pattern (C). Center distance ratio was higher in apoE3 than in apoE4 mice and in males than in females, suggesting a more anxiety-like profile in apoE4 mice and females (D). ApoE4 females also displayed higher center velocity than apoE3 females (E). Data are presented as mean ± SEM. ApoE3 male CNT (n = 9), apoE3 male PM (n = 10), apoE3 female CNT (n = 11), apoE3 female PM (n = 10), apoE4 male CNT (n = 10), apoE4 male PM (n = 11), apoE4 female CNT (n = 11), apoE4 female PM (n = 10). *p ≤ 0.05, **p < 0.01. Abbreviations: ApoE3 mice (E3), ApoE4 mice (E4), Control (CNT), Genotype (Gen), Particulate matter (PM), Treatment (Ttm).

treatment groups were examined separately, CNT males travelled a greater distance than CNT females during both the 0–10 min [$F_{1,68}$= 17.765, p < 0.001, η_p^2= 0.207] and 10–20 min intervals [$F_{1,68}$= 19.690, p < 0.001, η_p^2= 0.225]. In the PM-exposed group, males also traveled a greater distance than females, but this difference was restricted to the 10–20 min interval [$F_{1,68}$= 3.968, p = 0.050, η_p^2= 0.055].

The center-related parameters were used as indicators of anxiety-like behavior. ApoE3 mice showed more frequent entries into the center than apoE4 mice [$F_{1,75}$ = 13.587, p < 0.001, η_p^2= 0.153], and males also showed a higher number of center entries than females [$F_{1,75}$= 6.208, p = 0.015, η_p^2= 0.076]. Time spent in the center was also higher in apoE3 than in apoE4 mice [$F_{1,75}$= 8.926, p = 0.004, η_p^2= 0.106]. Similarly, the ratio between distance traveled in the center and total distance was higher in apoE3 than in apoE4 mice [$F_{1,68}$= 13.603, p < 0.001, η_p^2= 0.167], and higher in males than in females [$F_{1,68}$= 5.433, p = 0.023, η_p^2= 0.074], with a trend toward a Genotype × Sex × Treatment interaction [$F_{1,68}$= 3.282, p = 0.074, η_p^2= 0.046] (Fig. 4D). For center velocity, a significant Genotype × Sex interaction was observed [$F_{1,75}$= 4.023, p = 0.049, η_p^2= 0.051], with apoE4 females showing higher velocity than apoE3 females [$F_{1,75}$= 4.139, p = 0.045, η_p^2= 0.052] (Fig. 4E). Overall, these findings suggest that apoE4 mice displayed a more anxiety-like profile than apoE3 mice, while females showed reduced center-directed exploration compared with males.

Although body weight at PND70 was negatively associated with total distance traveled in the OFT after controlling for genotype, sex, and treatment (partial r = −0.302, p = 0.010), adjustment for body weight

in the factorial model did not alter the statistical conclusions. The effects of genotype and sex remained significant, whereas treatment and all interaction effects remained non-significant.

3.4. Three-chamber social test reveals subgroup-specific patterns in social behavior in apoE3 mice

During the habituation phase, total distance traveled (Fig. 5A) and mean velocity (Fig. 5B) showed significant effects of Genotype (distance: [$F_{1,76}$=5.503, $p = 0.022$, η_p^2=0.068], velocity: [$F_{1,76}$ =4.438, $p = 0.038$, η_p^2=0.055]) and Sex (distance:[$F_{1,76}$ =21.330, $p < 0.001$, η_p^2=0.219], velocity: [$F_{1,76}$ =16.982, $p < 0.001$, η_p^2=0.183]), with apoE3 mice traveling a greater distance and moving at a higher velocity than apoE4 mice, and males showing higher locomotor activity than females. Moreover, animals spent more time in both lateral chambers than in the central chamber [$F_{2,75}$= 233.961, $p < 0.001$, η_p^2= 0.862]; importantly, no significant differences were observed between the left and right chambers, indicating the absence of baseline side preference. Although a significant Time × Genotype interaction [$F_{2,75}$= 4.666, $p = 0.012$, η_p^2= 0.111] was detected and localized to the central chamber [$F_{1,76}$= 7.988, $p = 0.006$, η_p^2= 0.095], this effect did not reflect side bias and therefore did not compromise the interpretation of the subsequent phases.

The same genotype- and sex-dependent locomotor profile was also observed during the sociability and social novelty phases, with apoE3 mice showing higher total distance traveled and mean velocity than

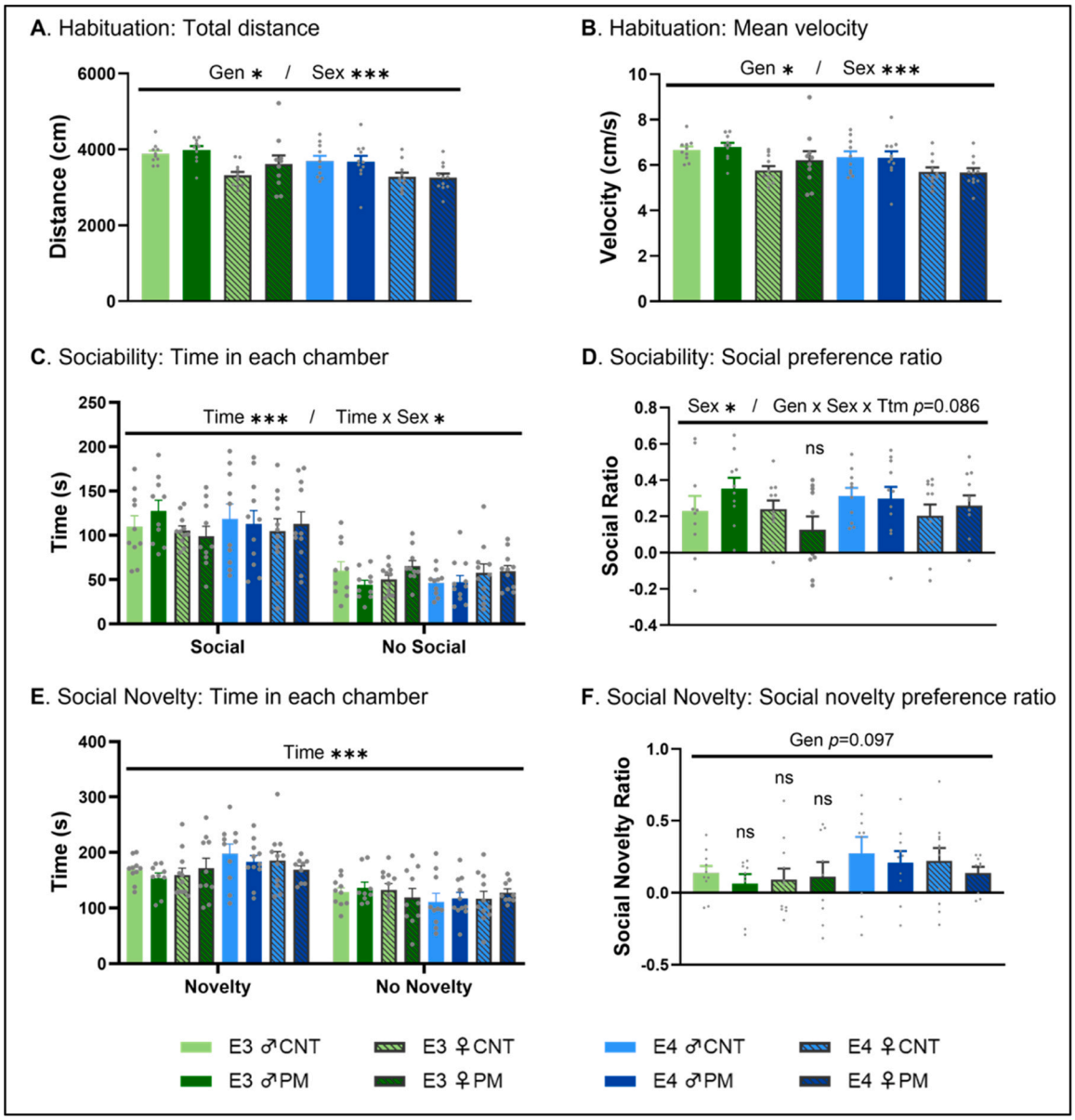


Fig. 5. Three-Chamber Social Test. During the habituation phase, apoE3 mice showed higher locomotor activity than apoE4 mice, and males showed higher locomotor activity than females, as reflected by greater distance traveled (A) and higher mean velocity (B). During the sociability phase, mice spent significantly more time in the social chamber than in the non-social chamber, with males showing greater social exploration than females (C). ApoE3 PM-treated females did not show a significant preference for the social stimulus (D). During the social novelty phase, mice spent significantly more time in the novel social chamber than in the familiar chamber (E). ApoE3 PM-treated males, as well as apoE3 females under both control and PM-exposed conditions, did not show a significant preference for the novel social stimulus (F). Data are presented as mean ± SEM. ApoE3 male CNT (n = 10), apoE3 male PM (n = 9–10), apoE3 female CNT (n = 11), apoE3 female PM (n = 10), apoE4 male CNT (n = 10), apoE4 male PM (n = 11), apoE4 female CNT (n = 11), apoE4 female PM (n = 9–11). *p ≤ 0.05, ***p < 0.001, ns=non-significant. Abbreviations: ApoE3 mice (E3), ApoE4 mice (E4), Control (CNT), Genotype (Gen), Particulate matter (PM).

apoE4 mice, and males displaying higher locomotor activity than females.

During the sociability phase, mice showed a robust preference for the social stimulus, spending significantly more time in the social than in the non-social chamber [$F_{1,76}$= 130.012, $p < 0.001$, η_p^2= 0.631] (Fig. 5C). This effect was modulated by sex, as indicated by a significant Time × Sex interaction [$F_{1,76}$= 4.946, $p = 0.029$, η_p^2= 0.061]. Follow-up Bonferroni-corrected comparisons confirmed significant sociability in both males and females [$F_{1,76}$= 90.677 and 43.149, respectively, $p < 0.001$, η_p^2= 0.544 and 0.362, respectively]; however, males spent more time in the social chamber than females [$F_{1,76}$= 5.584, $p = 0.021$, η_p^2= 0.068], with no sex difference in the non-social chamber [$F_{1,76}$= 3.687, $p = 0.059$]. Consistently, analysis of the social preference ratio revealed a significant effect of Sex [$F_{1,76}$= 4.283, $p = 0.042$, η_p^2= 0.053], together with a trend toward a Genotype × Sex × Treatment interaction [$F_{1,76}$= 3.028, $p = 0.086$, η_p^2= 0.038], suggesting that social preference may be differentially modulated across genotype, sex, and treatment conditions. To further characterize preference within each experimental group, the social preference ratio was tested against zero. In apoE3 PM-treated females, social preference did not reach statistical significance (t_9=1.745, $p = 0.057$) (Fig. 5D). However, because the Genotype × Sex × Treatment interaction was not significant and no direct between-treatment difference was detected, this within-group result should not be interpreted as evidence of a PM-induced sociability deficit.

During the social novelty phase, mice spent significantly more time in the novel social chamber than in the familiar social chamber [$F_{1,73}$= 32.417, $p < 0.001$, η_p^2= 0.308] (Fig. 5E), indicating an overall preference for social novelty. Analysis of the social novelty preference ratio showed only a trend toward a Genotype effect [$F_{1,73}$= 2.832, $p = 0.097$, η_p^2= 0.037], with no significant treatment-related effects or interactions. One-sample *t* tests showed that social novelty preference did not reach statistical significance in apoE3 PM-treated males (t_8=0.980, $p = 0.178$) or in apoE3 females under either control (t_{10}=1.161, $p = 0.136$) or PM-exposed conditions (t_9=1.589, $p = 0.073$) (Fig. 5F). Although these within-group patterns may suggest attenuated social preference in some PM-exposed subgroups, they do not demonstrate differences between treatments. In the absence of significant treatment-related effects or interactions, these observations should be considered exploratory and warrant further investigation of possible subgroup-specific responses to PM.

3.5. APOE genotype modulates sucrose preference dynamics without inducing anhedonia-like behavior

One-sample t-tests against the 50% chance level confirmed a preference for sucrose over tap water in all groups, both for daily sucrose preference values and for the mean intake across the 3-day testing period, indicating preserved sucrose preference and no evidence of anhedonia-like behavior. Nevertheless, sucrose preference varied significantly across testing days [$F_{2,73}$= 25.358, $p < 0.001$, η_p^2= 0.410], with a significant Day × Genotype interaction [$F_{2,73}$= 10.993, $p < 0.001$, η_p^2 = 0.231], indicating genotype-dependent differences in the temporal profile of sucrose preference (Fig. 6A). Simple-effects analyses showed that apoE4 mice exhibited higher sucrose preference than apoE3 mice on Day 1 [$F_{1,74}$= 5.650, $p = 0.020$, η_p^2= 0.071] and Day 3 [$F_{1,74}$= 7.985, $p = 0.006$, η_p^2= 0.097]. No significant interactions involving sex or treatment were detected.

To determine whether these differences reflected changes in general drinking behavior, total fluid intake was also analyzed. Total intake varied significantly across days [$F_{2,73}$= 33.050, $p < 0.001$, η_p^2= 0.475], but no significant interactions involving genotype, sex, or treatment were observed. These findings indicate that the genotype-dependent differences in sucrose preference were not attributable to differences in overall fluid consumption.

3.6. APOE genotype influences Morris water maze performance without consistent evidence of spatial memory deficits

Body weight showed a significant main effect of Day [$F_{2,75}$= 14.094, $p < 0.001$, η_p^2= 0.273] and a significant Day × Genotype interaction [$F_{2,75}$= 14.390, $p < 0.001$, η_p^2= 0.277], indicating that body weight changed over time and that this temporal pattern differed by genotype. A significant between-subject effect of Sex was also observed [$F_{1,76}$= 579.482, $p < 0.001$, η_p^2= 0.884], reflecting the expected higher body weight in males compared with females. The Day × Genotype interaction was driven by a transient reduction in body weight in apoE4 mice on Day 5 ($p < 0.001$), whereas apoE3 mice showed relatively stable body weight across the assessment period. Body weight on MWM Day 1 was not significantly associated with either mean swim velocity (partial r = 0.075, $p = 0.508$) or mean latency to reach the platform (partial r = 0.114, $p = 0.312$) during acquisition after controlling for genotype, sex, and treatment.

During the acquisition phase, RM-ANOVA revealed a significant main effect of Day for distance traveled [$F_{4,73}$= 94.129, $p < 0.001$, η_p^2= 0.838], latency to reach the platform [$F_{4,73}$= 79.395, $p < 0.001$, η_p^2= 0.813] (Fig. 7A), and swim velocity [$F_{4,73}$= 75.030, $p < 0.001$, η_p^2= 0.804], indicating progressive improvement across training days. Significant Day × Genotype interactions were observed for both distance traveled [$F_{4,73}$= 4.470, $p = 0.003$, η_p^2= 0.197] and latency [$F_{4,73}$= 2.981, $p = 0.024$, η_p^2= 0.140]. Follow-up simple-effects analyses showed significant genotype differences on each acquisition day for both parameters, with apoE4 mice traveling shorter distances and reaching the platform faster than apoE3 mice, indicating better acquisition performance.

In the 4-h probe trial, apoE3 mice showed lower locomotor/exploratory activity than apoE4 mice, as reflected by reduced distance traveled

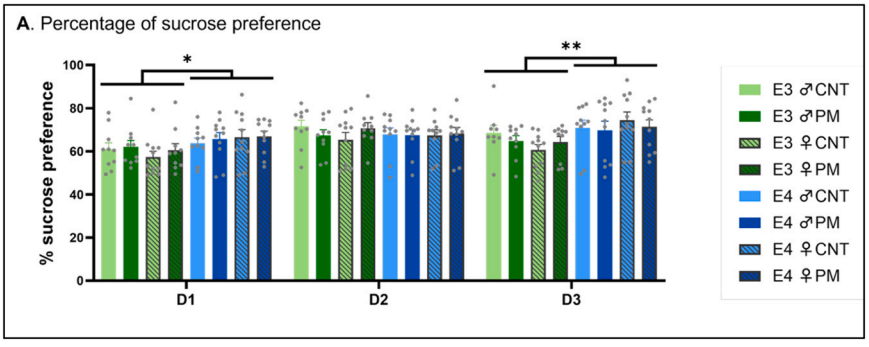


Fig. 6. Sucrose Preference Test. All experimental groups showed sucrose preference above chance level, indicating preserved hedonic behavior, but apoE4 mice displayed higher sucrose preference than apoE3 mice on Days 1 and 3 (A). Data are presented as mean ± SEM. ApoE3 male CNT (n = 10), apoE3 male PM (n = 10), apoE3 female CNT (n = 11), apoE3 female PM (n = 10), apoE4 male CNT (n = 10), apoE4 male PM (n = 11), apoE4 female CNT (n = 11), apoE4 female PM (n = 11). *p ≤ 0.05, **p < 0.01. Abbreviations: ApoE3 mice (E3), ApoE4 mice (E4), Control (CNT), Particulate matter (PM).

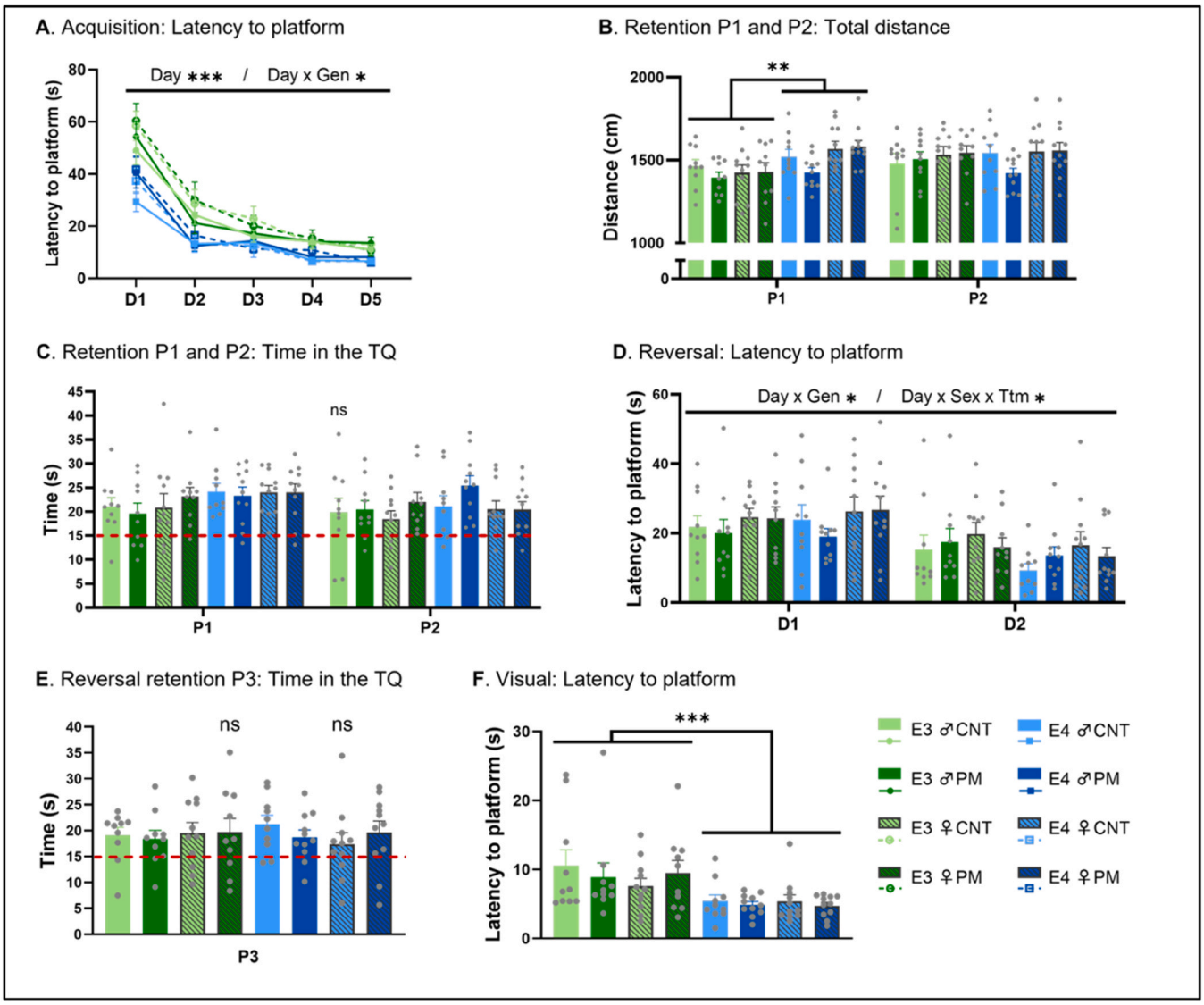


Fig. 7. Morris Water Maze Test. Animals progressively improved performance across training days, with apoE4 mice reaching the platform faster than apoE3 mice (A). ApoE3 mice showed reduced locomotor/exploratory activity compared with apoE4 mice during P1, whereas no differences were found in P2 (B). All groups spent more time in the TQ than expected by chance during P1, whereas apoE3 control males failed to show significant retention during P2 (C). Animals improved reversal performance from Day 1 to Day 2, with apoE4 mice showing a greater reduction in latency than apoE3 mice. PM-treated males did not significantly improve reversal performance across days (D). Most groups spent more time in the TQ than expected by chance in the P3, although apoE3 PM-treated females and apoE4 control females did not reach significance (E). ApoE3 mice showed longer latencies than apoE4 mice in the visual phase, indicating genotype-dependent differences in visible-platform performance (F). Data are presented as mean ± SEM. ApoE3 male CNT (n = 10), apoE3 male PM (n = 10), apoE3 female CNT (n = 11), apoE3 female PM (n = 10), apoE4 male CNT (n = 10), apoE4 male PM (n = 11), apoE4 female CNT (n = 11), apoE4 female PM (n = 11). *p ≤ 0.05, **p < 0.01, ***p < 0.001, ns=non-significant. Abbreviations: ApoE3 mice (E3), ApoE4 mice (E4), Control (CNT), Day (D), Particulate matter (PM), Probe (P).

[$F_{1,76}$= 10.344, $p = 0.002$, η_p^2= 0.120] (Fig. 7B) and swim velocity [$F_{1,76}$= 10.344, $p = 0.002$, η_p^2= 0.120]. However, no significant group differences were detected in 4-h spatial memory, although a trend toward a Genotype effect was observed for time spent in the TQ [$F_{1,76}$= 3.712, $p = 0.058$]. One-sample *t*-tests against chance level further showed that all groups spent significantly more time in the TQ than expected by chance, indicating preserved short-term spatial memory (Fig. 7C).

In the 72-h probe trial, no significant group differences were observed in total distance, swim velocity, or long-term spatial memory performance. However, one-sample *t*-tests against chance level showed that apoE3 control males did not spend significantly more time in the TQ than expected by chance (t_9=1.652, $p = 0.067$), suggesting a possible attenuation of long-term memory retention in this subgroup (Fig. 7C).

During reversal learning, animals improved from Day 1 to Day 2, as shown by reduced distance traveled [$F_{1,76}$= 33.308, $p < 0.001$, η_p^2= 0.305] and shorter latency to reach the platform [$F_{1,76}$= 42.013, $p < 0.001$, η_p^2= 0.356] (Fig. 7D), indicating successful acquisition of the new platform location. For latency, a significant Day × Genotype interaction was observed [$F_{1,76}$= 4.259, $p = 0.042$, η_p^2= 0.053], with both genotypes improving across reversal days but apoE4 mice showing a more pronounced reduction in latency. Reversal performance was also modulated by sex and treatment, as indicated by significant Day × Sex × Treatment interactions for distance traveled [$F_{1,76}$= 4.751, $p = 0.032$, η_p^2= 0.059] and latency [$F_{1,76}$= 3.950, $p = 0.050$, η_p^2= 0.049]. Follow-up analyses showed that PM-treated males did not significantly reduce either distance traveled [$F_{1,76}$= 1.737, $p = 0.192$] or latency [$F_{1,76}$= 2.505, $p = 0.118$] from Day 1 to Day 2. No significant effects were detected for swim velocity, suggesting that the observed differences were not driven by altered motor performance.

In the reversal probe trial, no significant between-group differences were observed in total distance traveled, swim velocity, new TQ, time spent in the former TQ, or the flexibility index (time in new TQ – old TQ). One-sample *t*-tests against chance level showed that most groups spent significantly more time in the new TQ than expected by chance. However, this effect did not reach significance in apoE3 PM-treated females (t_9=1.787, $p = 0.054$) or apoE4 control females (t_{10}=1.099, $p = 0.149$) (Fig. 7E), suggesting weaker retention of the new platform location in these subgroups.

In the visual phase, significant Genotype effects were observed for distance traveled [$F_{1,76}$= 14.087, $p < 0.001$, η_p^2= 0.156], latency to reach the visible platform [$F_{1,76}$= 16.820, $p < 0.001$, η_p^2= 0.181] (Fig. 7F), and swim velocity [$F_{1,74}$= 4.107, $p = 0.046$, η_p^2= 0.053]. ApoE3 mice showed longer latencies, traveled greater distances, and swam at higher velocities than apoE4 mice, indicating poorer visible-platform performance in this genotype. These findings suggest that sensorimotor, motivational, or visual factors may contribute to genotype-related differences in MWM performance; therefore, the genotype effects observed during acquisition and reversal should not be interpreted exclusively as impaired spatial learning.

3.7. Hippocampal gene-expression responses to PM exposure are mainly shaped by APOE genotype

In the HPC, gene-expression changes were primarily driven by genotype, with additional sex- and treatment-dependent effects emerging in selected molecular pathways. Within synaptic plasticity and post-synaptic organization markers, *Creb1* (Fig. 8A) and *Dlg4* (Fig. 8B) showed significant main effects of Genotype, with higher expression in apoE4 than apoE3 mice [*Creb1*: $F_{1,30}$= 7.225, $p = 0.012$, η_p^2= 0.194; *Dlg4*: $F_{1,31}$= 4.250, $p = 0.048$, η_p^2= 0.121]. Regarding glutamatergic neurotransmission, *Grin2a* was significantly affected by Genotype, with higher expression in apoE3 than apoE4 mice [$F_{1,32}$= 5.731, $p = 0.023$, η_p^2= 0.152] (Fig. 8C), while Grin2b showed a trend toward a Genotype effect [$F_{1,32}$= 3.687, $p = 0.064$]. The vesicular glutamate transporter *Vglut1* also showed a nominal Genotype effect, with higher expression in apoE3 than apoE4 mice [$F_{1,31}$= 10.600, $p = 0.003$, η_p^2= 0.255], together with trends for Sex [$F_{1,31}$= 3.638, $p = 0.066$] and Treatment [$F_{1,31}$= 3.692, $p = 0.064$], and a significant Sex × Treatment interaction [$F_{1,31}$= 4.850, $p = 0.035$, η_p^2= 0.135] (Fig. 8D). Simple-effects analyses indicated that the sex effect was significant under control conditions [$F_{1,31}$= 8.197, $p = 0.007$, η_p^2= 0.209], with higher *Vglut1* expression in males than females. In males, a significant Treatment effect was also observed [$F_{1,31}$= 8.252, $p = 0.007$, η_p^2= 0.210], with PM-treated males showing reduced *Vglut1* expression compared with control males. In contrast, no significant effects were observed for the GABAergic markers *Gabra1*, *Gad1*, or *Gad2*, nor for the serotonin receptors *Htr1a* and *Htr2c*.

For markers related to astrocytic and microglial activation, *Gfap* showed a significant Genotype effect, with higher expression in apoE4 than apoE3 mice [$F_{1,31}$= 6.370, $p = 0.017$, η_p^2= 0.170] (Fig. 8E); whereas *Iba1* showed trends toward Genotype [$F_{1,31}$= 3.024, $p = 0.092$] and Sex × Treatment effects [$F_{1,31}$= 3.081, $p = 0.089$]. Myelin-associated genes were also strongly modulated by Genotype, with apoE3 mice showing lower expression than apoE4 mice for both *Mog* (Fig. 8F) [$F_{1,31}$= 11.133, $p = 0.002$, η_p^2= 0.264] and *Plp1* (Fig. 8G) [$F_{1,31}$= 9.710, $p = 0.004$, η_p^2= 0.239]. *Plp1* also showed a trend toward a Genotype × Sex × Treatment interaction [$F_{1,31}$= 3.516, p = 0.070].

Within oxidative-stress-related genes, *Gpx1* showed a significant Genotype effect, with higher expression in apoE4 than apoE3 mice [$F_{1,32}$= 8.285, $p = 0.007$, η_p^2= 0.206], together with a trend toward a Genotype × Treatment interaction [$F_{1,32}$= 3.473, $p = 0.072$] (Fig. 8H). *Hmox1* exhibited the strongest Genotype effect among all targets, with higher expression in apoE3 than apoE4 mice [$F_{1,31}$= 22.648, $p < 0.001$, η_p^2= 0.422] (Fig. 8I). In addition, *Hmox1* showed a significant Sex effect, with higher expression in males than females [$F_{1,31}$= 5.762, $p = 0.023$, η_p^2= 0.157], as well as a significant Sex × Treatment interaction [$F_{1,31}$= 5.324, $p = 0.028$, η_p^2= 0.147] and a trend toward a Genotype × Sex × Treatment interaction [$F_{1,31}$= 3.060, $p = 0.090$]. Simple-effects analyses showed that the sex effect was significant in control animals [$F_{1,31}$= 10.755, $p = 0.003$, η_p^2= 0.258], with higher expression in males than females. Treatment showed only a trend in males [$F_{1,31}$= 3.835, $p = 0.059$]. In contrast, *Sod2* was not significantly affected by genotype, sex, treatment, or their interactions.

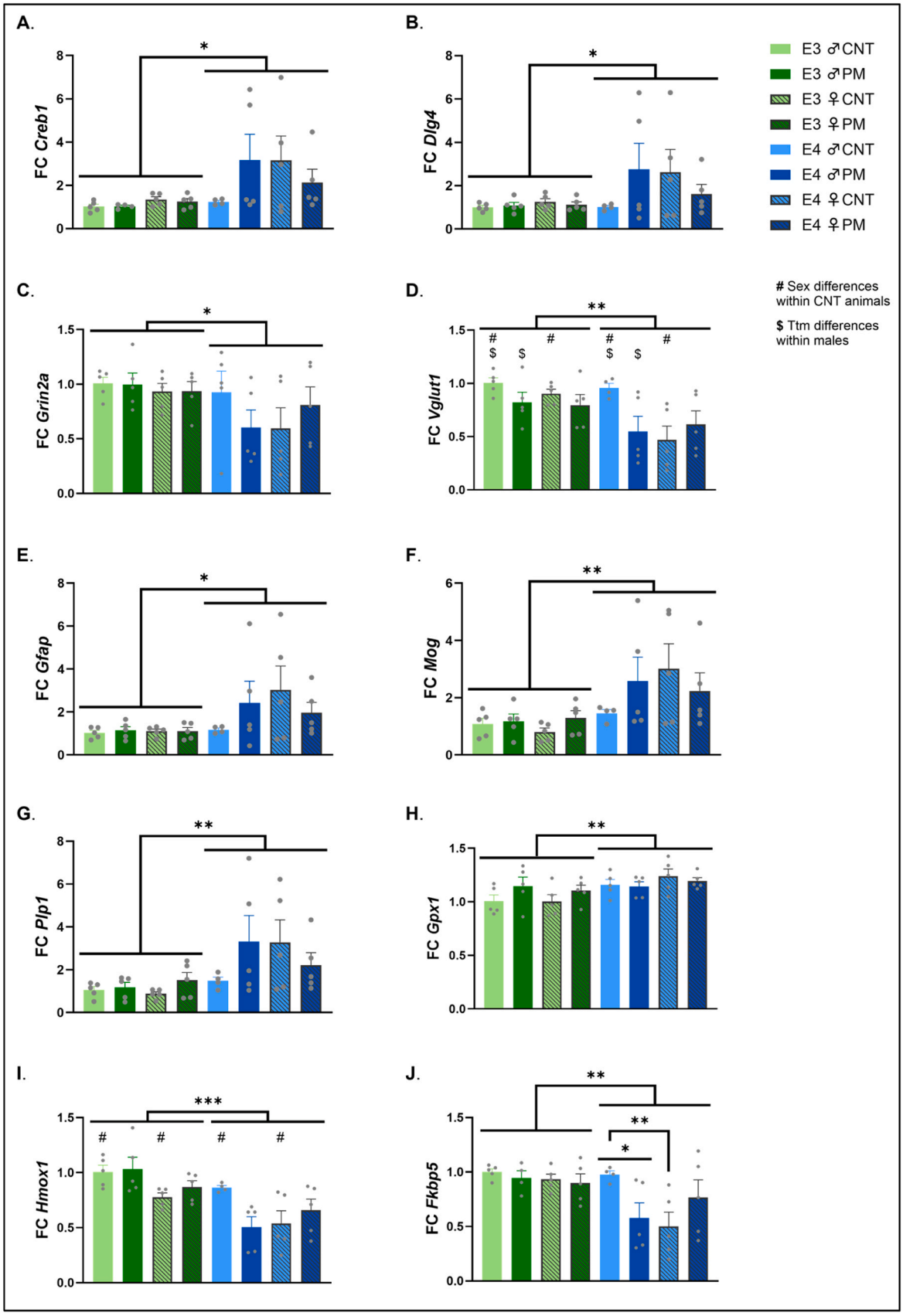
Finally, within stress-response and glucocorticoid-signaling markers, *Fkbp5* showed a significant main effect of Genotype, with higher expression in apoE3 than apoE4 mice [$F_{1,30}$= 10.684, $p = 0.003$, η_p^2= 0.263] (Fig. 8J). In addition, *Fkbp5* showed a significant Sex × Treatment interaction [$F_{1,30}$= 5.539, $p = 0.025$, η_p^2= 0.156] and a significant Genotype × Sex × Treatment interaction [$F_{1,30}$= 4.858, $p = 0.035$, η_p^2= 0.139], indicating that treatment-related modulation depended on both sex and genotype. Simple-effects analyses indicated that the sex effect was significant only under control conditions [$F_{1,30}$= 6.942, $p = 0.013$, η_p^2= 0.188], with higher expression in males than females, an effect mainly driven by particularly low levels in apoE4 females. In males, a significant Treatment effect was also observed [$F_{1,30}$= 4.612, $p = 0.040$, η_p^2= 0.133], with PM-treated males showing lower *Fkbp5* expression than control males, particularly within the apoE4 genotype. Genotype differences were detected in PM-exposed males [$F_{1,30}$= 5.972, $p = 0.021$, η_p^2= 0.166] and control females [$F_{1,30}$= 9.299, $p = 0.005$, η_p^2= 0.237]. Further decomposition showed that sex differences were restricted to apoE4 control animals [$F_{1,30}$= 10.059, $p = 0.003$, η_p^2= 0.251]. Treatment effects were mainly present in apoE4 males [$F_{1,30}$= 7.096, $p = 0.012$, η_p^2= 0.191], where PM exposure reduced *Fkbp5* expression, while a trend in apoE4 females suggested the opposite pattern [$F_{1,30}$= 3.506, $p = 0.071$]. No significant effects were observed for *Nr3c1*.

3.8. PM exposure selectively modulates striatal synaptic and dopaminergic/striatal markers

In the STR, gene-expression changes were more restricted than in the HPC and were mainly detected in synaptic, dopaminergic/striatal, and glutamatergic-related markers. Among synaptic markers, *Creb1* showed a significant Sex × Treatment interaction [$F_{1,30}$= 7.041, $p = 0.013$, η_p^2= 0.190] (Fig. 9A). Simple-effects analyses indicated that PM-treated males showed higher *Creb1* expression than PM-treated females [$F_{1,30}$= 6.193, $p = 0.019$, η_p^2= 0.171]. Treatment effects were also significant in males [$F_{1,30}$= 4.644, $p = 0.039$, η_p^2= 0.134], reflecting higher *Creb1* expression in PM-treated males than in control males. *Dlg4* showed significant Genotype × Treatment [$F_{1,30}$= 4.344, $p = 0.046$, η_p^2= 0.126] and Sex × Treatment interactions [$F_{1,30}$= 4.465, $p = 0.043$, η_p^2= 0.130] (Fig. 9B). Although decomposition of the Genotype × Treatment interaction did not reveal significant simple effects, the Sex × Treatment interaction was driven by higher expression in PM-treated males than in PM-treated females [$F_{1,30}$= 4.927, $p = 0.034$, η_p^2= 0.141].

Regarding dopaminergic/striatal markers, *Drd2* (Fig. 9C) and *Ppp1r1b* (Fig. 9D) showed significant Genotype effects, with lower expression in apoE3 than in apoE4 mice [*Drd2*: $F_{1,31}$= 7.092, $p = 0.012$, η_p^2= 0.186; *Ppp1r1b*: $F_{1,32}$= 8.412, $p = 0.007$, η_p^2= 0.208]. *Drd2* also showed a trend toward a Genotype × Treatment interaction [$F_{1,31}$= 3.520, $p = 0.070$], apparently driven by apoE4 mice, in which PM-exposed animals tended to show lower expression than controls. Within glutamatergic-related markers, *Vglut1* showed a significant main effect of Treatment [$F_{1,29}$= 4.934, $p = 0.034$, η_p^2= 0.145], with PM-exposed animals showing overall higher expression than controls (Fig. 9E). However, this pattern was less evident in apoE4 males, where control and PM-exposed groups showed comparable levels. In contrast, *Grin2a*, *Grin2b*, and *Grm5* were not significantly affected by genotype, sex, treatment, or their interactions.

No significant effects were detected for GABAergic markers (*Gabra1*, *Gad1*, *Gad2*), serotonin receptors (*Htr1a*, *Htr2c*), or markers related to



(caption on next page)

Fig. 8. Hippocampal gene expression. *Creb1* (A) and *Dlg4* (B) expression were higher in apoE4 than in apoE3 mice. *Grin2a* expression was reduced in apoE4 mice compared with apoE3 mice (C). *Vglut1* expression showed genotype-dependent differences together with sex- and treatment-related modulation (D). *Gfap* (E), *Mog* (F), and *Plp1* (G) expression were higher in apoE4 than in apoE3 mice. *Gpx1* expression was increased in apoE4 mice compared with apoE3 mice (H). *Hmox1* expression was higher in apoE3 than in apoE4 mice, and control males showed higher expression than control females (I). *Fkbp5* expression was reduced in PM-exposed apoE4 males compared with control apoE4 males; control apoE4 males exhibited higher expression than control apoE4 females, and apoE3 mice presented higher expression than apoE4 mice (J). Data are presented as fold change (FC) relative to apoE3 male controls and expressed as mean ± SEM. n = 4/5. *p ≤ 0.05, **p < 0.01, ***p < 0.001; # Sex differences within CNT animals, $ Treatment differences within males (both comparisons were derived from the Sex × Ttm interaction). Reported p-values are nominal and were not adjusted across the complete set of gene-expression targets. Bonferroni adjustment was applied to post hoc comparisons following significant interaction effects. Abbreviations: ApoE3 mice (E3), ApoE4 mice (E4), Control (CNT), Particulate matter (PM), Treatment (Ttm).

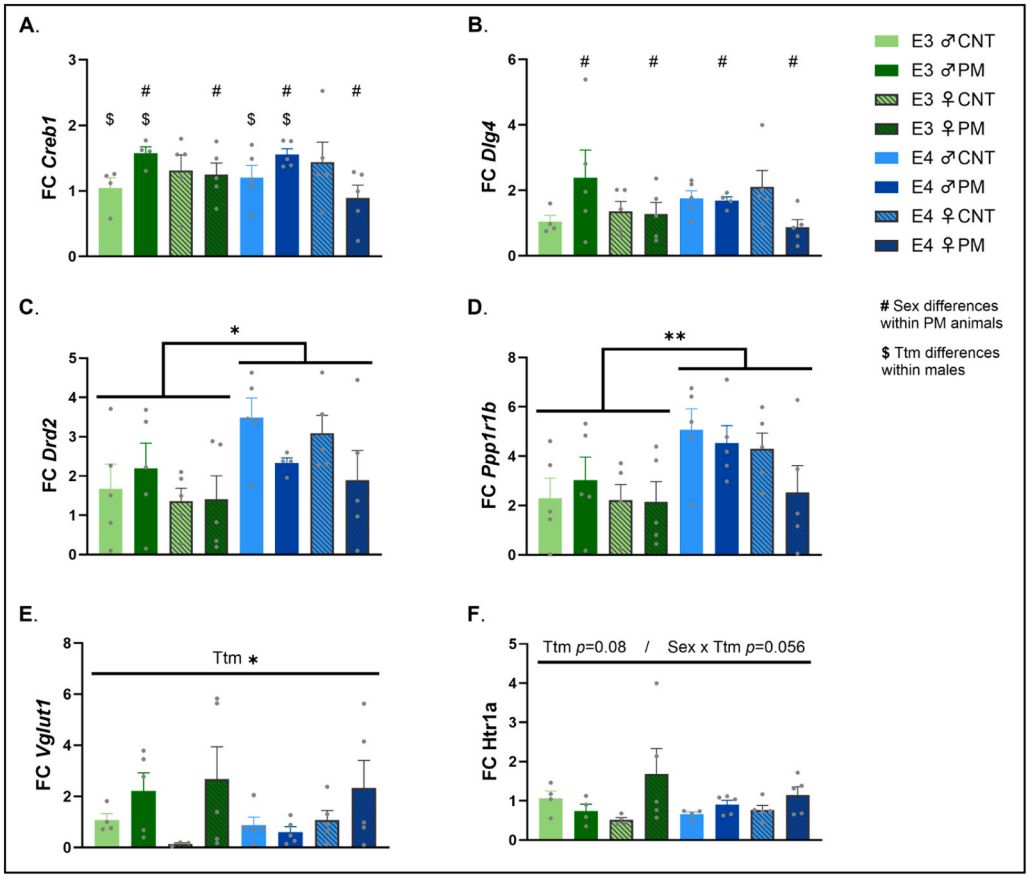


Fig. 9. Striatal gene expression. *Creb1* expression showed sex- and treatment-dependent modulation, with PM-exposed males displaying higher expression than PM-exposed females, and PM exposure increasing expression in males (A). *Dlg4* expression also showed sex-dependent modulation under PM exposure, with PM-exposed males exhibiting higher expression than PM-exposed females (B). *Drd2* (C) and *Ppp1r1b* (D) showed higher expression in apoE4 than in apoE3 mice. *Vglut1* expression was increased in PM-exposed animals compared with controls (E). *Htr1a* expression tended to be higher in PM-treated animals than in controls, particularly in apoE3 females (F). Data are presented as fold change (FC) relative to apoE3 male controls and expressed as mean ± SEM. n = 4/5. *p ≤ 0.05, **p < 0.01; # Sex differences within PM animals, $ Treatment differences within males (both comparisons were derived from the Sex × Ttm interaction). Reported p-values are nominal and were not adjusted across the complete set of gene-expression targets. Bonferroni adjustment was applied to post hoc comparisons following significant interaction effects. Abbreviations: ApoE3 mice (E3), ApoE4 mice (E4), Control (CNT), Particulate matter (PM), Treatment (Ttm).

glial activation, myelination, and stress signaling (*Gfap*, *Iba1*, *Mog*, *Plp1*, *Fkbp5*, *Nr3c1*), although *Htr1a* showed trends toward a Treatment effect [$F_{1,28}$= 3.293, p = 0.080] and a Sex × Treatment interaction [$F_{1,28}$= 3.988, p = 0.056] (Fig. 9F).

4. Discussion

The present study shows that early postnatal exposure to PM induces long-lasting behavioral and molecular alterations in young adult humanized apoE-TR mice, but these effects do not emerge as a generalized PM-driven phenotype. Instead, the data reveal a complex pattern in which *APOE* genotype represents the main organizing factor of adult behavioral and gene-expression profiles, while PM exposure produces selective, sex- and region-dependent modifications. This is particularly relevant because PND4–14 represents a highly sensitive developmental period characterized by ongoing neurogenesis, synaptogenesis, gliogenesis, and circuit refinement (Semple et al., 2013; Zeiss, 2021), supporting the relevance of this model for investigating the long-term consequences of an environmental insult during a critical window of brain maturation. In humans, however, these developmental processes span late gestation and the early postnatal period, resulting in distinct exposure routes across developmental stages. During pregnancy, maternal exposure to PM may affect the fetus through oxidative stress and placental alterations (Grevendonk et al., 2016; Janssen et al., 2012), while combustion-derived particles can reach the placenta and translocate to the fetal circulation and organs (Bongaerts et al., 2022; Bové

et al., 2019). After birth, inhalation becomes a direct exposure route for the developing infant. By contrast, in our model, exposure occurred exclusively during the postnatal period, with direct inhalation throughout the entire exposure window.

A central finding of this work is that apoE3 and apoE4 mice displayed clearly divergent adult phenotypes: apoE3 mice generally showed higher locomotor and exploratory activity, whereas apoE4 mice exhibited reduced center-directed exploration in the OFT, suggesting a more anxiety-like profile, alongside a broad hippocampal transcriptional reorganization. Together, these findings indicate that APOE genotype is a major determinant of adult behavioral and molecular phenotypes. Importantly, the effects of PM exposure were highly context-dependent. Rather than inducing broad deterioration, early-life PM exposure selectively modified behavioral domains and molecular markers. This pattern suggests that developmental PM exposure may act less as a uniform neurotoxic insult and more as a modifier of genotype- and sex-dependent developmental programming.

Body-weight effects were transient and mainly restricted to weaning and post-weaning growth. The greater weight gain observed in apoE3 males and, more markedly, in PM-exposed apoE3 females may be consistent with catch-up growth contributing to body-weight normalization. This aligns with our previous developmental study, in which PM exposure reduced female weight gain between PND14 and PND28 (Rodulfo-Cárdenas et al., 2026), and with Liu et al. (2019), who reported reduced body weight after early postnatal PM exposure at PND28 but not at PND60. Overall, these findings suggest that early postnatal PM exposure may transiently disrupt growth trajectories without producing stable alterations by young adulthood.

Similarly, Rotarod acquisition revealed genotype-, sex-, and treatment-dependent differences in the temporal dynamics of motor performance. Nonetheless, these effects were restricted to specific trials and were not maintained during the test phase. Thus, early postnatal PM exposure did not produce a robust impairment in motor coordination or motor learning, but rather subtle changes in initial task adaptation. This is consistent with developmental PM studies reporting no major motor alterations after gestational/postnatal exposure to diesel-related particles (Morris-Schaffer et al., 2019b; Nway et al., 2017), although motor outcomes may vary according to particle composition, exposure paradigm, age at assessment, and sex (Cory-Slechta et al., 2018). Importantly, the absence of consistent motor alterations indicates that subsequent behavioral effects in the OFT, 3CST, and MWM are unlikely to reflect a generalized motor deficit.

Across the OFT and all phases of the 3CST, apoE3 mice consistently displayed higher locomotor activity than apoE4 mice, whereas males were generally more active than females. This stable exploratory phenotype is relevant for interpreting subsequent behavioral outcomes, particularly in the MWM, where performance may be influenced by non-cognitive factors. In the OFT, animals showed progressive habituation to the novel environment, and this temporal profile was modulated by sex and treatment, suggesting that PM exposure may subtly alter the expression of sex-dependent exploratory responses. Beyond locomotion, center-related measures indicated a clear anxiety-like profile, with apoE4 mice and females showing reduced center-directed exploration. The apoE4-related profile is consistent with previous findings in female APOE-TR mice (Siegel et al., 2010). However, the effects of developmental PM exposure on anxiety-like behavior remain heterogeneous across studies, with some reporting anxiety-like behavior in juvenile rodents shortly after exposure (Li et al., 2024; Liu et al., 2019; Vanbrabant et al., 2024; Wang et al., 2024), whereas others found no significant alterations in adults (Morris-Schaffer et al., 2019a; Sobolewski et al., 2018). These findings suggest that anxiety-like outcomes following developmental PM exposure depend on dose, particle composition, sex, and age at behavioral assessment, with effects potentially being more evident shortly after exposure than in young adulthood.

The 3CST showed robust overall sociability and social novelty preference, although exploratory one-sample analyses revealed subgroup-specific patterns. Social preference did not reach significance in PM-exposed apoE3 females, while social novelty preference did not reach significance in PM-exposed apoE3 males or in apoE3 females under either treatment condition. Previous studies have similarly reported alterations in sociability and/or social novelty preference in young adult animals after prenatal and postnatal exposure to diesel exhaust (Chang et al., 2018; Win-Shwe et al., 2016) or $PM_{2.5}$ (Church et al., 2018). Moreover, complementary social-interaction paradigms have shown reduced reciprocal social behavior, particularly in exposed males (Chang et al., 2018; Church et al., 2018). However, not all postnatal exposure studies found social alterations, as social conditioned place preference was unaffected in some models (Morris-Schaffer et al., 2019a; Sobolewski et al., 2018). These findings support that social behavior is a sensitive outcome after developmental exposure to PM, while the exploratory patterns observed here suggest that possible long-term vulnerability in apoE3 subgroups warrants further investigation, particularly given that *APOE* ε3 is the most prevalent allele in the general population (Liu et al., 2013a).

In the SPT, all groups showed sucrose preference above chance level, indicating no evidence of anhedonia-like behavior. Nevertheless, apoE4 mice displayed higher sucrose preference than apoE3 mice on specific testing days, revealing a genotype-dependent temporal profile that was independent of total fluid intake. While Liu et al. (2019) reported increased depression-like behavior using the forced swimming test in rats exposed to the highest $PM_{2.5}$ dose (10 mg/kg.b.w) at 60 days of age, the present results suggest that early postnatal PM exposure did not induce persistent anhedonia-like alterations in young adulthood, although *APOE* genotype may influence reward-related or motivational behavior under basal conditions. Given the limited literature on developmental PM exposure and anhedonia-like outcomes, further studies are needed to clarify its long-term effects on reward-related behavior.

Regarding the MWM, apoE4 mice consistently reached the platform faster and traveled shorter distances than apoE3 mice during acquisition and reversal learning. Notwithstanding, these differences were not accompanied by robust impairments in short- or long-term spatial memory. Moreover, the strong genotype effect observed during the visual phase indicates that apoE4 performance cannot be interpreted solely as enhanced spatial learning. Rather, these findings point to broader genotype-dependent differences in task performance, potentially involving search strategy, motivational state, or stress responsivity. In this context, the more anxiety-like profile observed in apoE4 mice in the OFT may influence how animals engage with stressful testing environments. Previous studies reported impaired MWM performance shortly after postnatal $PM_{2.5}$ exposure, with effects no longer evident by young adulthood (Liu et al., 2019), suggesting that PM-related cognitive alterations may be temporally restricted. In addition, cognitive outcomes in APOE-TR models are highly heterogeneous and influenced by genetic background, colony origin, age, and experimental conditions (van Heuvelen et al., 2024). Although apoE4 is associated with cognitive decline later in life, preserved or even enhanced performance has been reported in young apoE4 animals under specific conditions (Moreau et al., 2013; Siegel et al., 2010), supporting the hypothesis of age-dependent pleiotropic effects, potentially promoting compensatory mechanisms during early adulthood (Tuminello and Han, 2011). Thus, the present findings reflect complex apoE4-related differences in behavioral strategy rather than cognitive impairment per se.

The exploratory candidate-gene analyses identified nominal expression differences involving synaptic, glutamatergic, glial, myelin-related, redox, and stress-response markers. In the HPC, *APOE* genotype was the main driver of gene-expression differences. ApoE4 mice showed increased expression of genes related to synaptic plasticity and postsynaptic organization (*Creb1*, *Dlg4*), with reduced expression of markers related to glutamatergic neurotransmission (*Vglut1*, *Grin2a*). *CREB1* is a transcription factor critically involved in synaptic plasticity and memory formation (Benito and Barco, 2010), whereas *DLG4*

encodes PSD-95, a major postsynaptic scaffolding protein that organizes glutamatergic synapses and contributes to NMDA/AMPA receptor stabilization and signaling (Coley and Gao, 2017). *VGLUT1* encodes the principal presynaptic vesicular glutamate transporter responsible for glutamate loading into synaptic vesicles (Eriksen et al., 2020), while *GRIN2A* encodes the GluN2A subunit of NMDA receptors, which contributes to glutamatergic neurotransmission and synaptic plasticity (Franchini et al., 2020). The coexistence of reduced glutamatergic markers with increased synaptic-organization markers may reflect circuit remodeling or adaptive synaptic reorganization rather than widespread synaptic loss. This agrees with increased *DLG4* expression in postmortem HPC tissue from human APOE4 carriers without AD (Sinclair and Love, 2017), and altered glutamatergic synaptic function, including reduced hippocampal VGLUT1 levels and disrupted Reelin-dependent NMDA receptor trafficking, in APOE4-TR mice (Chen et al., 2010; Liraz et al., 2013; Sun et al., 2017). Beyond the genotype effect, PM exposure further reduced *Vglut1* expression in males, consistent with previous evidence that developmental PM exposure can alter hippocampal glutamatergic neurochemistry, particularly in male rodents (Allen et al., 2014a, 2014b; Cory-Slechta et al., 2019). This suggests that early postnatal PM exposure may be associated with sex-dependent changes in presynaptic glutamatergic regulation.

This synaptic/glutamatergic profile was accompanied by increased expression of the myelin-related genes (*Plp1*, *Mog)*, together with higher *Gfap* expression in apoE4 mice. *PLP1* encodes the major structural proteolipid protein of CNS myelin, which contributes to myelin compaction and maintenance (Simons et al., 2002), whereas *MOG* encodes an oligodendrocyte-specific glycoprotein widely associated with oligodendrocyte maturation and mature myelinating states (Peschl et al., 2017). In parallel, *GFAP* encodes the principal intermediate filament protein of astrocytes and is widely considered a marker of astroglial reactivity (Eng et al., 2000). Importantly, increased transcription of myelin-associated genes does not necessarily imply more efficient or structurally preserved myelination. Young APOE4-TR mice exhibit impaired myelination and thinner myelin sheaths associated with altered cholesterol handling and oligodendrocyte dysfunction (Blanchard et al., 2022), and PLP overexpression can disrupt PLP/cholesterol trafficking and promote hypomyelination (Simons et al., 2002). Thus, the increased expression of myelin-related genes may reflect an early compensatory response in apoE4 mice that may help preserve function during young adulthood but could become insufficient later in life as myelin plasticity and repair capacity decline (Chapman and Hill, 2019). The parallel increase in *Gfap* may indicate astroglial reactivity, which could be particularly relevant because astrocytes play a central role in lipid transport and metabolic support to oligodendrocytes (Camargo et al., 2017). Given that myelin maintenance critically depends on proper cholesterol handling, these exploratory findings support the notion that APOE4 may induce early myelin-associated remodeling processes in young adulthood.

The apoE4-associated hippocampal profile was further characterized by increased *Gpx1* expression together with reduced *Hmox1* and *Fkbp5* levels. *GPX1* encodes glutathione peroxidase-1, a major antioxidant enzyme involved in peroxide detoxification and cellular redox defense (Handy and Loscalzo, 2022), whereas *HMOX1* encodes the stress-inducible enzyme heme oxygenase-1, commonly associated with oxidative-inflammatory responses (Ryter and Choi, 2015). In agreement with the reduced *Hmox1* expression, *APOE4* has been associated with decreased nuclear Nrf2 signaling and reduced expression of Nrf2-dependent antioxidant targets (Graeser et al., 2011). In parallel, *FKBP5* encodes a glucocorticoid-responsive co-chaperone involved in stress-response regulation and hypothalamic–pituitary–adrenal axis modulation, and is highly sensitive to environmental stressors through gene–environment and epigenetic mechanisms (Zannas et al., 2015). Thus, the specific reduction of *Fkbp5* in PM-exposed apoE4 males suggests that early-life PM exposure may interact with *APOE* genotype and sex to modulate stress-response regulatory pathways. Overall, the combined profile does not suggest a uniform oxidative-inflammatory state, but rather possible selective redox and stress-response regulation associated with apoE4-related hippocampal remodeling.

Compared with the HPC, STR gene-expression changes were more restricted. PM exposure primarily affected markers related to plasticity and excitatory input, increasing *Creb1* expression in males and *Vglut1* expression overall, while *Dlg4* was higher in PM-exposed males than in PM-exposed females. Together with the opposite *Vglut1* pattern observed in the HPC, these findings suggest that early postnatal PM exposure may modulate glutamatergic regulation in a region- and sex-dependent manner. Given the distinct functional roles of the HPC and STR, these divergent responses may reflect region-specific adaptations in excitatory neurotransmission across cognitive versus motivational circuits. In parallel, apoE4 mice showed higher *Drd2* and *Ppp1r1b* expression than apoE3 mice. *DRD2* encodes the dopamine D2 receptor, a key regulator of striatal dopaminergic signaling, motor output, reward processing, and motivational behavior (Gallo, 2019), whereas *PPP1R1B* encodes DARPP-32, a central integrator of dopamine- and glutamate-dependent signaling (Svenningsson et al., 2004). These genotype-dependent differences may point to APOE-related modulation of dopaminergic/striatal signaling, which could contribute to basal differences in exploratory or motivational behavior between apoE3 and apoE4 mice.

The present study has several limitations. First, a single PM dose and exposure regimen was used, precluding dose–response assessments. Additionally, although the amount of PM introduced into the chamber was known, the actual airborne concentration, its temporal variation, particle-size distribution, and physicochemical characteristics of the aerosol reaching the animals were not directly measured in situ. The actual exposure was therefore expected to be lower than the calculated theoretical maximum and to vary during the session because of continuous airflow, chamber leakage, sedimentation, and deposition on chamber surfaces. Individual ventilation and pulmonary deposition in the pups were also not quantified. Consequently, the nominal chamber loading cannot be converted into an actual inhaled or deposited dose, limiting dose interpretation. The absence of in situ aerosol characterization also restricts exact replication of the exposure atmosphere and direct quantitative comparison with studies reporting measured time-weighted concentrations, aerodynamic particle-size distributions, or deposited doses. Nevertheless, the use of a standardized and extensively characterized reference material, together with the detailed reporting of the chamber configuration, nebulization conditions, and dose-calculation assumptions, facilitates methodological reproducibility. Future studies should incorporate real-time or gravimetric monitoring of airborne PM, aerodynamic particle-size characterization, and assessment of deposited dose to improve dosimetric interpretation and cross-study comparability.

Second, although PND4–14 broadly overlaps with late gestation and early postnatal development in humans in terms of selected brain-maturation processes, cross-species differences in developmental timing and the absence of a maternal–placental exposure pathway and fetal dosimetry preclude direct extrapolation to human prenatal exposure. Third, the absence of a concurrent wild-type control group precludes direct assessment of how apoE3 and apoE4 mice differ from the background strain, although the study was specifically designed to evaluate APOE-dependent susceptibility. Finally, molecular analyses were exploratory, based on a pre-selected, mechanistically motivated panel of candidate genes, and limited to mRNA expression in selected brain regions. No multiplicity correction was applied across the complete set of gene-expression targets. Therefore, the possibility of false-positive findings cannot be excluded. The molecular results should consequently be considered hypothesis-generating and require replication and functional validation. Moreover, protein-level changes, cell-type-specific effects, and functional consequences at the synaptic or circuit level cannot be inferred.

Overall, the current findings indicate that early postnatal PM exposure does not induce a uniform or generalized neurotoxic phenotype, but

rather selectively modulates specific dimensions of social behavior, task adaptation, and behavioral engagement in a subgroup-dependent manner. At the molecular level, these effects were accompanied by selective circuit-related changes involving glutamatergic, synaptic, and stress-response pathways. However, *APOE* genotype emerged as the main organizer of adult behavioral and molecular profiles. In young apoE4 mice, the combination of preserved behavioral performance and broad HPC transcriptional reorganization may reflect adaptive or compensatory network remodeling rather than overt dysfunction. This interpretation is consistent with the proposed antagonistic pleiotropic effects of *APOE4* (Tuminello and Han, 2011), whereby mechanisms that may support neural efficiency or behavioral adaptation early in life may later become maladaptive with aging. Conversely, the apoE3 profile may point toward reduced motivational salience or task engagement rather than cognitive impairment per se. Together, these findings support the notion that *APOE* genotype not only modulates vulnerability to environmental insults but also shapes baseline neurodevelopmental organization and the way in which environmental exposures are behaviorally and molecularly expressed during early adulthood. Therefore, the long-term consequences of developmental PM exposure may be better understood as selective alterations in neurodevelopmental calibration emerging through complex interactions between environmental exposure, genotype, sex, and circuit-specific brain organization.

5. Conclusions

Early postnatal PM exposure induced long-lasting behavioral and molecular alterations in humanized apoE mice, but these effects were highly selective and strongly influenced by *APOE* genotype and sex rather than reflecting a generalized neurotoxic phenotype. Across both behavioral and molecular domains, *APOE* genotype emerged as the principal factor shaping adult outcomes, whereas PM exposure mainly modulated specific aspects of social behavior, task adaptation, and glutamatergic- and stress-related pathways. Notably, young apoE4 mice exhibited a broad HPC transcriptional reorganization accompanied by preserved behavioral performance, supporting the idea that *APOE4* may promote adaptive or compensatory mechanisms during early adulthood. These findings highlight the importance of considering genetic susceptibility when evaluating the long-term consequences of developmental air-pollution exposure. Future studies should determine whether the molecular adaptations observed in young apoE4 animals remain beneficial across the lifespan or instead contribute to increased vulnerability as aging and neurodegenerative processes emerge.

CRediT authorship contribution statement

Rocío Rodulfo-Cárdenas: Writing – original draft, Methodology, Investigation, Formal analysis, Data curation, Conceptualization, Visualization. **Judit Biosca-Brull:** Investigation, Writing – review & editing. **Séfora Barberà-Parada:** Investigation, Writing – review & editing. **Raquel Gabaldón-Díaz:** Investigation, Writing – review & editing. **Diego Ruiz-Sobremazas:** Methodology, Writing – review & editing. **Jordi Blanco:** Writing – review & editing, Supervision. **Maria Cabré:** Writing – review & editing, Methodology, Supervision, Validation. **José L. Domingo:** Writing – review & editing. **Caridad López-Granero:** Writing – review & editing, Conceptualization. **Fernando Sánchez-Santed:** Writing – review & editing, Conceptualization. **Maria Teresa Colomina:** Writing – review & editing, Supervision, Project administration, Investigation, Funding acquisition, Conceptualization, Methodology, Validation, Visualization.

Declaration of Generative AI and AI-assisted technologies in the writing process

During the preparation of this work, the author used ChatGPT5 in order to assist with grammar and language correction. After using this tool, the author reviewed and edited the content as needed and takes full responsibility for the content of the published article.

Funding

This work was supported by the Spanish Ministry of Science, Innovation and Universities (MICIU, Spain) (References: PID2020-113812RB-C31, PID2020-113812RB-C32, PID2020-113812RB-C33) (Grant reference: PRE2021-097136).

Declaration of Competing Interest

The authors declare that they have no known competing financial interests or personal relationships that could have appeared to influence the work reported in this paper.

Acknowledgments

The authors would like to thank Dr. Celeste de Paolo, Esperanza Chernichero and Juan Valencia for their skillful technical support with the care of animals. We also acknowledge the Department of Biochemistry and Biotechnology of Tarragona for providing access to the QuantStudio™ 5 Real-Time PCR System.

Appendix A. Supporting information

Supplementary data associated with this article can be found in the online version at doi:10.1016/j.neuro.2026.103580.

Data availability

Data will be made available on request.

References

Alemany, S., Vilor-Tejedor, N., García-Esteban, R., Bustamante, M., Dadvand, P., Esnaola, M., Mortamais, M., Forns, J., van Drooge, B.L., Álvarez-Pedrerol, M., Grimalt, J.O., Rivas, I., Querol, X., Pujol, J., Sunyer, J., 2018. Traffic-related air pollution, APOE ε4 status, and neurodevelopmental outcomes among school children enrolled in the BREATHE project (Catalonia, Spain). Environ. Health Perspect. 126, 087001. https://doi.org/10.1289/EHP2246.

Allen, J.L., Liu, X., Pelkowski, S., Palmer, B., Conrad, K., Oberdörster, G., Weston, D., Mayer-Pröschel, M., Cory-Slechta, D.A., 2014a. Early postnatal exposure to ultrafine particulate matter air pollution: persistent ventriculomegaly, neurochemical disruption, and glial activation preferentially in male mice. Environ. Health Perspect. 122, 939–945. https://doi.org/10.1289/EHP.1307984.

Allen, J.L., Liu, X., Weston, D., Prince, L., Oberdörster, G., Finkelstein, J.N., Johnston, C. J., Cory-Slechta, D.A., 2014b. Developmental exposure to concentrated ambient ultrafine particulate matter air pollution in mice results in persistent and sex-dependent behavioral neurotoxicity and glial activation. Toxicol. Sci. 140, 160–178. https://doi.org/10.1093/toxsci/kfu059.

Altmann, A., Tian, L., Henderson, V.W., Greicius, M.D., 2014. Sex modifies the APOE-related risk of developing Alzheimer's disease. Ann. Neurol. 75, 563. https://doi.org/10.1002/ANA.24135.

Anagnostaras, S.G., Gale, G.D., Fanselow, M.S., 2001. Hippocampus and contextual fear conditioning: recent controversies and advances. Hippocampus 11, 8–17. https://doi.org/10.1002/1098-1063(2001)11:1<8::AID-HIPO1015>3.0.CO;2-7.

Applied Biosystems, 2008. Guide to Performing Relative Quantitation of Gene Expression Using Real-Time Quantitative PCR [WWW Document]. URL. https://documents.thermofisher.com/TFS-Assets/LSG/manuals/cms_042380.pdf (accessed 4.30.26).

Báez-Mendoza, R., Schultz, W., 2013. The role of the striatum in social behavior. Front. Neurosci. 7, 233. https://doi.org/10.3389/FNINS.2013.00233.

Basaure, P., Guardia-Escote, L., Biosca-Brull, J., Blanco, J., Cabré, M., Peris-Sampedro, F., Sánchez-Santed, F., Domingo, J.L., Colomina, M.T., 2019. Exposure to chlorpyrifos at different ages triggers APOE genotype-specific responses in social behavior, body weight and hypothalamic gene expression. Environ. Res. 178, 108684. https://doi.org/10.1016/J.ENVRES.2019.108684.

Benito, E., Barco, A., 2010. CREB's control of intrinsic and synaptic plasticity: implications for CREB-dependent memory models. Trends Neurosci. 33, 230–240. https://doi.org/10.1016/J.TINS.2010.02.001.

Blanchard, J.W., Akay, L.A., Davila-Velderrain, J., von Maydell, D., Mathys, H., Davidson, S.M., Effenberger, A., Chen, C.Y., Maner-Smith, K., Hajjar, I., Ortlund, E. A., Bula, M., Agbas, E., Ng, A., Jiang, X., Kahn, M., Blanco-Duque, C., Lavoie, N., Liu, L., Reyes, R., Lin, Y.T., Ko, T., R'Bibo, L., Ralvenius, W.T., Bennett, D.A., Cam, H. P., Kellis, M., Tsai, L.H., 2022. APOE4 impairs myelination via cholesterol

dysregulation in oligodendrocytes. Nature 7937 (611), 769–779. https://doi.org/10.1038/S41586-022-05439-W.
Block, M.L., Calderón-Garcidueñas, L., 2009. Air pollution: mechanisms of neuroinflammation and CNS disease. Trends Neurosci. 32, 506–516. https://doi.org/10.1016/J.TINS.2009.05.009.
Bongaerts, E., Lecante, L.L., Bové, H., Roeffaers, M.B.J., Ameloot, M., Fowler, P.A., Nawrot, T.S., 2022. Maternal exposure to ambient black carbon particles and their presence in maternal and fetal circulation and organs: an analysis of two independent population-based observational studies. Lancet Planet. Health 6, e804. https://doi.org/10.1016/S2542-5196(22)00200-5.
Bové, H., Bongaerts, E., Slenders, E., Bijnens, E.M., Saenen, N.D., Gyselaers, W., Van Eyken, P., Plusquin, M., Roeffaers, M.B.J., Ameloot, M., Nawrot, T.S., 2019. Ambient black carbon particles reach the fetal side of human placenta. Nat. Commun. 1 (10), 3866. https://doi.org/10.1038/S41467-019-11654-3.
Calderón-Garcidueñas, L., De La Monte, S.M., 2017. Apolipoprotein E4, gender, body mass index, inflammation, insulin resistance, and air pollution interactions: recipe for Alzheimer's disease development in Mexico City young females. J. Alzheimers Dis. 58, 613. https://doi.org/10.3233/JAD-161299.
Calderón-Garcidueñas, L., Hernández-Luna, J., Aiello-Mora, M., Brito-Aguilar, R., Evelson, P.A., Villarreal-Ríos, R., Torres-Jardón, R., Ayala, A., Mukherjee, P.S., 2023. APOE peripheral and brain impact: APOE4 carriers accelerate their alzheimer continuum and have a high risk of suicide in PM2.5 polluted cities. Biomolecules 13, 927. https://doi.org/10.3390/BIOM13060927.
Camargo, N., Goudriaan, A., van Deijk, A.L.F., Otte, W.M., Brouwers, J.F., Lodder, H., Gutmann, D.H., Nave, K.A., Dijkhuizen, R.M., Mansvelder, H.D., Chrast, R., Smit, A. B., Verheijen, M.H.G., 2017. Oligodendroglial myelination requires astrocyte-derived lipids. PLoS. Biol. 15. https://doi.org/10.1371/JOURNAL.PBIO.1002605.
Chang, Y.C., Cole, T.B., Costa, L.G., 2018. Prenatal and early-life diesel exhaust exposure causes autism-like behavioral changes in mice. Part. Fibre Toxicol. 15. https://doi.org/10.1186/S12989-018-0254-4.
Chapman, T.W., Hill, R.A., 2019. Myelin plasticity in adulthood and aging. Neurosci. Lett. 715, 134645. https://doi.org/10.1016/J.NEULET.2019.134645.
Chen, Y., Durakoglugil, M.S., Xian, X., Herz, J., 2010. ApoE4 reduces glutamate receptor function and synaptic plasticity by selectively impairing ApoE receptor recycling. Proc. Natl. Acad. Sci. U. S. A. 107, 12011–12016. https://doi.org/10.1073/PNAS.0914984107.
Church, J.S., Tijerina, P.B., Emerson, F.J., Coburn, M.A., Blum, J.L., Zelikoff, J.T., Schwartzer, J.J., 2018. Perinatal exposure to concentrated ambient particulates results in autism-like behavioral deficits in adult mice. Neurotoxicology 65, 231. https://doi.org/10.1016/J.NEURO.2017.10.007.
Clougherty, J.E., 2009. A growing role for gender analysis in air pollution epidemiology. Environ. Health Perspect. 118, 167. https://doi.org/10.1289/EHP.0900994.
Cohen, A.J., Brauer, M., Burnett, R., Anderson, H.R., Frostad, J., Estep, K., Balakrishnan, K., Brunekreef, B., Dandona, L., Dandona, R., Feigin, V., Freedman, G., Hubbell, B., Jobling, A., Kan, H., Knibbs, L., Liu, Y., Martin, R., Morawska, L., Pope, C.A., Shin, H., Straif, K., Shaddick, G., Thomas, M., van Dingenen, R., van Donkelaar, A., Vos, T., Murray, C.J.L., Forouzanfar, M.H., 2017. Estimates and 25-year trends of the global burden of disease attributable to ambient air pollution: an analysis of data from the Global Burden of Diseases Study 2015. Lancet 389, 1907–1918. https://doi.org/10.1016/S0140-6736(17)30505-6.
Coley, A.A., Gao, W.J., 2017. PSD95: a synaptic protein implicated in schizophrenia or autism? Prog. Neuropsychopharmacol. Biol. Psychiatry 82, 187. https://doi.org/10.1016/J.PNPBP.2017.11.016.
Cory-Slechta, D.A., Allen, J.L., Conrad, K., Marvin, E., Sobolewski, M., 2018. Developmental exposure to low level ambient ultrafine particle air pollution and cognitive dysfunction. Neurotoxicology 69, 217–231. https://doi.org/10.1016/j.neuro.2017.12.003.
Cory-Slechta, D.A., Sobolewski, M., Marvin, E., Conrad, K., Merrill, A., Anderson, T., Jackson, B.P., Oberdorster, G., 2019. The impact of inhaled ambient ultrafine particulate matter on developing brain: potential importance of elemental contaminants. Toxicol. Pathol. 47, 976–992. https://doi.org/10.1177/0192623319878400.
Costa, L.G., Aschner, M., Vitalone, A., Syversen, T., Soldin, O.P., 2004. Developmental neuropathology of environmental agents. Annu. Rev. Pharmacol. Toxicol. 44, 87–110. https://doi.org/10.1146/ANNUREV.PHARMTOX.44.101802.121424.
Costa, L.G., Cole, T.B., Dao, K., Chang, Y.C., Coburn, J., Garrick, J.M., 2020. Effects of air pollution on the nervous system and its possible role in neurodevelopmental and neurodegenerative disorders. Pharmacol. Ther. 210, 107523. https://doi.org/10.1016/J.PHARMTHERA.2020.107523.
Costa, L.G., Cole, T.B., Dao, K., Chang, Y.C., Garrick, J.M., 2019. Developmental impact of air pollution on brain function. Neurochem. Int. 131, 104580. https://doi.org/10.1016/J.NEUINT.2019.104580.
Dean, D.C., Jerskey, B.A., Chen, K., Protas, H., Thiyyagura, P., Roontiva, A., O'Muircheartaigh, J., Dirks, H., Waskiewicz, N., Lehman, K., Siniard, A.L., Turk, M. N., Hua, X., Madsen, S.K., Thompson, P.M., Fleisher, A.S., Huentelman, M.J., Deoni, S.C.L., Reiman, E.M., 2014. Brain differences in infants at differential genetic risk for late-onset Alzheimer disease a cross-sectional imaging study. JAMA Neurol. 71, 11. https://doi.org/10.1001/JAMANEUROL.2013.4544.
Deidda, G., Pierucci, M., Crunelli, V., Di Giovanni, G., 2021. 5-HT/GABA interaction in neurodevelopment and plasticity. Prog. Brain Res. 259, 287–317. https://doi.org/10.1016/BS.PBR.2021.01.009.
Dong, Z., Bai, Y., Wu, X., Li, H., Gong, B., Howland, J.G., Huang, Y., He, W., Li, T., Wang, Y.T., 2013. Hippocampal long-term depression mediates spatial reversal learning in the Morris water maze. Neuropharmacology 64, 65–73. https://doi.org/10.1016/J.NEUROPHARM.2012.06.027.
Dose, J., Huebbe, P., Nebel, A., Rimbach, G., 2016. APOE genotype and stress response - a mini review. Lipids Health Dis. 15. https://doi.org/10.1186/S12944-016-0288-2.
Eng, L.F., Ghirnikar, R.S., Lee, Y.L., 2000. Glial fibrillary acidic protein: GFAP-thirty-one years (1969-2000). Neurochem. Res. 25, 1439–1451. https://doi.org/10.1023/A:1007677003387.
EPA, 2002. Consideration of the FQPA Safety Factor and Other Uncertainty Factors in Cumulative Risk Assessment of Chemicals Sharing a Common Mechanism of Toxicity | US EPA [WWW Document]. URL. https://www.epa.gov/pesticide-science-and-assessing-pesticide-risks/consideration-fqpa-safety-factor-and-other (accessed 11.3.25).
Eriksen, J., Li, F., Edwards, R.H., 2020. The mechanism and regulation of vesicular glutamate transport: coordination with the synaptic vesicle cycle. Biochim. Biophys. Acta Biomembr. 1862, 183259. https://doi.org/10.1016/J.BBAMEM.2020.183259.
Feng, S., Gao, D., Liao, F., Zhou, F., Wang, X., 2016. The health effects of ambient PM2.5 and potential mechanisms. Ecotoxicol. Environ. Saf. 128, 67–74. https://doi.org/10.1016/J.ECOENV.2016.01.030.
Foley, K.E., Hewes, A.A., Garceau, D.T., Kotredes, K.P., Carter, G.W., Sasner, M., Howell, G.R., 2022. The APOEε3/ε4 genotype drives distinct gene signatures in the cortex of young mice. Front. Aging Neurosci. 14. https://doi.org/10.3389/fnagi.2022.838436.
Franchini, L., Carrano, N., Di Luca, M., Gardoni, F., 2020. Synaptic GluN2A-containing NMDA receptors: from physiology to pathological synaptic plasticity. Int. J. Mol. Sci. 21, 1538. https://doi.org/10.3390/IJMS21041538.
Gallo, E.F., 2019. Disentangling the diverse roles of dopamine D2 receptors in striatal function and behavior. Neurochem. Int. 125, 35. https://doi.org/10.1016/J.NEUINT.2019.01.022.
Gonzalez, C.A., Choquette, S.J., 2021. Certificate of Analysis of Standard Reference Material® 2787 [WWW Document]. URL. https://tsapps.nist.gov/srmext/certificates/2787.pdf (accessed 1.15.26).
Graeser, A.C., Boesch-Saadatmandi, C., Lippmann, J., Wagner, A.E., Huebbe, P., Storm, N., Höppner, W., Wiswedel, I., Gardemann, A., Minihane, A.M., Döring, F., Rimbach, G., 2011. Nrf2-dependent gene expression is affected by the proatherogenic apoE4 genotype-studies in targeted gene replacement mice. J. Mol. Med. 89, 1027–1035. https://doi.org/10.1007/S00109-011-0771-1.
Graybiel, A.M., Grafton, S.T., 2015. The striatum: where skills and habits meet. Cold Spring Harb. Perspect. Biol. 7, a021691. https://doi.org/10.1101/CSHPERSPECT.A021691.
Grevendonk, L., Janssen, B.G., Vanpoucke, C., Lefebvre, W., Hoxha, M., Bollati, V., Nawrot, T.S., 2016. Mitochondrial oxidative DNA damage and exposure to particulate air pollution in mother-newborn pairs. Environ. Health 15, 10. https://doi.org/10.1186/S12940-016-0095-2.
Handy, D.E., Loscalzo, J., 2022. The role of glutathione peroxidase-1 in health and disease. Free. Radic. Biol. Med. 188, 146. https://doi.org/10.1016/J.FREERADBIOMED.2022.06.004.
Janssen, B.G., Munters, E., Pieters, N., Smeets, K., Cox, B., Cuypers, A., Fierens, F., Penders, J., Vangronsveld, J., Gyselaers, W., Nawrot, T.S., 2012. Placental mitochondrial DNA content and particulate air pollution during in utero life. Environ. Health Perspect. 120, 1346. https://doi.org/10.1289/EHP.1104458.
Jofre-Monseny, L., Minihane, A.M., Rimbach, G., 2008. Impact of apoE genotype on oxidative stress, inflammation and disease risk. Mol. Nutr. Food Res. 52, 131–145. https://doi.org/10.1002/MNFR.200700322.
Kang, Y.J., Tan, H.Y., Lee, C.Y., Cho, H., 2021. An air particulate pollutant induces neuroinflammation and neurodegeneration in human brain models. Adv. Sci. 8, 2101251. https://doi.org/10.1002/ADVS.202101251.
Kjelstrup, K.G., Tuvnes, F.A., Steffenach, H.A., Murison, R., Moser, E.I., Moser, M.B., 2002. Reduced fear expression after lesions of the ventral hippocampus. Proc. Natl. Acad. Sci. U. S. A. 99, 10825. https://doi.org/10.1073/PNAS.152112399.
Kleeberger, S.R., Ohtsuka, Y., 2005. Gene-particulate matter-health interactions. Toxicol. Appl. Pharmacol. 207, 276–281. https://doi.org/10.1016/J.TAAP.2005.03.025.
Kreitzer, A.C., Malenka, R.C., 2008. Striatal plasticity and basal ganglia circuit function. Neuron 60, 543. https://doi.org/10.1016/J.NEURON.2008.11.005.
Lenz, K.M., McCarthy, M.M., 2014. A starring role for microglia in brain sex differences. Neuroscientist 21, 306. https://doi.org/10.1177/1073858414536468.
Li, K., Liang, X., Liu, X., Geng, Y., Yan, J., Tian, L., Liu, H., Lai, W., Shi, Y., Xi, Z., Lin, B., 2024. Early-life exposure to PM2.5 leads to ASD-like phenotype in male offspring rats through activation of PI3K-AKT signaling pathway. Ecotoxicol. Environ. Saf. 274, 116222. https://doi.org/10.1016/J.ECOENV.2024.116222.
Liang, B., Zhang, L., Zhang, Y., Werner, C.T., Beacher, N.J., Denman, A.J., Li, Y., Chen, R., Gerfen, C.R., Barbera, G., Lin, D.T., 2022. Striatal direct pathway neurons play leading roles in accelerating rotarod motor skill learning. iScience 25, 104245. https://doi.org/10.1016/J.ISCI.2022.104245.
Liljeholm, M., O'Doherty, J.P., 2012. Contributions of the striatum to learning, motivation, and performance: an associative account. Trends Cogn. Sci. 16, 467. https://doi.org/10.1016/J.TICS.2012.07.007.
Liraz, O., Boehm-Cagan, A., Michaelson, D.M., 2013. ApoE4 induces Aβ42, tau, and neuronal pathology in the hippocampus of young targeted replacement apoE4 mice. Mol. Neurodegener. 8, 16. https://doi.org/10.1186/1750-1326-8-16.
Liu, C.C., Kanekiyo, T., Xu, H., Bu, G., 2013a. Apolipoprotein E and Alzheimer disease: risk, mechanisms and therapy. Nat. Rev. Neurol. 9, 106–118. https://doi.org/10.1038/NRNEUROL.2012.263.
Liu, C.C., Kanekiyo, T., Xu, H., Bu, G., 2013b. Apolipoprotein E and Alzheimer disease: risk, mechanisms, and therapy. Nat. Rev. Neurol. 9, 106. https://doi.org/10.1038/NRNEUROL.2012.263.
Liu, J., Yang, C., Yang, J., Song, X., Han, W., Xie, M., Cheng, L., Xie, L., Chen, H., Jiang, L., 2019. Effects of early postnatal exposure to fine particulate matter on

emotional and cognitive development and structural synaptic plasticity in immature and mature rats. Brain Behav. 9, e01453. https://doi.org/10.1002/BRB3.1453.
Liu, M.Y., Yin, C.Y., Zhu, L.J., Zhu, X.H., Xu, C., Luo, C.X., Chen, H., Zhu, D.Y., Zhou, Q. G., 2018. Sucrose preference test for measurement of stress-induced anhedonia in mice. Nat. Protoc. 7 (13), 1686–1698. https://doi.org/10.1038/S41596-018-0011-Z.
Miyoshi, E., Wietzikoski, E.C., Bortolanza, M., Boschen, S.L., Canteras, N.S., Izquierdo, I., Da Cunha, C., 2012. Both the dorsal hippocampus and the dorsolateral striatum are needed for rat navigation in the Morris water maze. Behav. Brain Res. 226, 171–178. https://doi.org/10.1016/J.BBR.2011.09.011.
Moreau, P.H., Bott, J.B., Zerbinatti, C., Renger, J.J., Kelche, C., Cassel, J.C., Mathis, C., 2013. ApoE4 confers better spatial memory than apoE3 in young adult hAPP-Yac/apoE-TR mice. Behav. Brain Res. 243, 1–5. https://doi.org/10.1016/J.BBR.2012.12.043.
Morris, R., 1984. Developments of a water-maze procedure for studying spatial learning in the rat. J. Neurosci. Methods 11, 47–60. https://doi.org/10.1016/0165-0270(84)90007-4.
Morris, R.G.M., Garrud, P., Rawlins, J.N.P., O'Keefe, J., 1982. Place navigation impaired in rats with hippocampal lesions. Nature 297, 681–683. https://doi.org/10.1038/297681A0.
Morris-Schaffer, K., Merrill, A., Jew, K., Wong, C., Conrad, K., Harvey, K., Marvin, E., Sobolewski, M., Oberdörster, G., Elder, A., Elder, A., Cory-Slechta, D.A., 2019a. Effects of neonatal inhalation exposure to ultrafine carbon particles on pathology and behavioral outcomes in C57BL/6J mice. Part. Fibre Toxicol. 16. https://doi.org/10.1186/s12989-019-0293-5.
Morris-Schaffer, K., Merrill, A.K., Wong, C., Jew, K., Sobolewski, M., Cory-Slechta, D.A., 2019b. Limited developmental neurotoxicity from neonatal inhalation exposure to diesel exhaust particles in C57BL/6 mice. Part. Fibre Toxicol. 16. https://doi.org/10.1186/s12989-018-0287-8.
Nway, N.C., Fujitani, Y., Hirano, S., Mar, O., Win-Shwe, T.T., 2017. Role of TLR4 in olfactory-based spatial learning activity of neonatal mice after developmental exposure to diesel exhaust origin secondary organic aerosol. Neurotoxicology 63, 155–165. https://doi.org/10.1016/J.NEURO.2017.10.001.
Office of Environmental Health Hazard Assessment, 2005. No Significant Risk Level (NSRL) for the Proposition 65 Carcinogen Naphthalene.
Pan, B., Chen, M., Zhang, X., Liang, S., Qin, X., Qiu, L., Cao, Q., Peng, R., Tao, S., Li, Z., Zhu, Y., Kan, H., Xu, Y., Ying, Z., 2020. Hypothalamic-pituitary-adrenal axis mediates ambient pm2.5 exposure-induced pulmonary inflammation. Ecotoxicol. Environ. Saf. 208, 111464. https://doi.org/10.1016/J.ECOENV.2020.111464.
Percie du Sert, N., Hurst, V., Ahluwalia, A., Alam, S., Avey, M.T., Baker, M., Browne, W. J., Clark, A., Cuthill, I.C., Dirnagl, U., Emerson, M., Garner, P., Holgate, S.T., Howells, D.W., Karp, N.A., Lazic, S.E., Lidster, K., MacCallum, C.J., Macleod, M., Pearl, E.J., Petersen, O.H., Rawle, F., Reynolds, P., Rooney, K., Sena, E.S., Silberberg, S.D., Steckler, T., Würbel, H., 2020. The ARRIVE guidelines 2.0: Updated guidelines for reporting animal research. PLoS. Biol. 18, e3000410. https://doi.org/10.1371/journal.pbio.3000410.
Peris-Sampedro, F., Guardia-Escote, L., Basaure, P., Cabré, M., Colomina, M.T., 2020. Improvement of APOE4-dependent non-cognitive behavioural traits by postnatal cholinergic stimulation in female mice. Behav. Brain Res. 384, 112552. https://doi.org/10.1016/J.BBR.2020.112552.
Peschl, P., Bradl, M., Höftberger, R., Berger, T., Reindl, M., 2017. Myelin oligodendrocyte glycoprotein: deciphering a target in inflammatory demyelinating diseases. Front. Immunol. 8, 529. https://doi.org/10.3389/FIMMU.2017.00529.
Pfaffl, M.W., 2001. A new mathematical model for relative quantification in real-time RT–PCR. Nucleic Acids Res. 29, e45. https://doi.org/10.1093/nar/29.9.e45.
Reverte, I., Klein, A.B., Ratner, C., Domingo, J.L., Colomina, M.T., 2012. Behavioral phenotype and BDNF differences related to apoE isoforms and sex in young transgenic mice. Exp. Neurol. 237, 116–125. https://doi.org/10.1016/J.EXPNEUROL.2012.06.015.
Riedel, B.C., Thompson, P.M., Diaz Brinton, R., Steroid, J., Mol, B., Author, B., 2016. Age, APOE and sex: triad of risk of Alzheimer's disease. J. Steroid Biochem. Mol. Biol. 160, 134. https://doi.org/10.1016/J.JSBMB.2016.03.012.
Rodier, P.M., 1994. Vulnerable periods and processes during central nervous system development. Environ. Health Perspect. 102, 121. https://doi.org/10.1289/EHP.94102121.
Rodulfo-Cárdenas, R., Biosca-Brull, J., Barberà-Parada, S., Gabaldón-Díaz, R., Ruiz-Sobremazas, D., Blanco, J., Cabré, M., Domingo, J.L., López-Granero, C., Sanchez-Santed, F., Colomina, M.T., 2026. Postnatal particulate matter exposure alters developmental milestones and brain gene expression in apoE transgenic mice in a sex- and genotype-dependent manner. Neurotoxicology 114, 103466. https://doi.org/10.1016/J.NEURO.2026.103466.
Rodulfo-Cárdenas, R., Ruiz-Sobremazas, D., Biosca-Brull, J., Cabré, M., Blanco, J., López-Granero, C., Sánchez-Santed, F., Colomina, M.T., 2023. The influence of environmental particulate matter exposure during late gestation and early life on the risk of neurodevelopmental disorders: a systematic review of experimental evidences. Environ. Res. 236, 116792. https://doi.org/10.1016/J.ENVRES.2023.116792.
Ruiz-Sobremazas, D., Rodulfo-Cárdenas, R., Ruiz-Coca, M., Morales-Navas, M., Teresa Colomina, M., López-Granero, C., Sánchez-Santed, F., Perez-Fernandez, C., 2023. Uncovering the link between air pollution and neurodevelopmental alterations during pregnancy and early life exposure: a systematic review. Neurosci. Biobehav. Rev. 152. https://doi.org/10.1016/J.NEUBIOREV.2023.105314.
Ryter, S.W., Choi, A.M.K., 2015. Targeting heme oxygenase-1/carbon monoxide for therapeutic modulation of inflammation. Transl. Res. 167, 7. https://doi.org/10.1016/J.TRSL.2015.06.011.
Sánchez-Soberón, F., Rovira, J., Sierra, J., Mari, M., Domingo, J.L., Schuhmacher, M., 2019. Seasonal characterization and dosimetry-assisted risk assessment of indoor particulate matter (PM10-2.5, PM2.5-0.25, and PM0.25) collected in different schools. Environ. Res. 175, 287–296. https://doi.org/10.1016/J.ENVRES.2019.05.035.
Semple, B.D., Blomgren, K., Gimlin, K., Ferriero, D.M., Noble-Haeusslein, L.J., 2013. Brain development in rodents and humans: identifying benchmarks of maturation and vulnerability to injury across species. Prog. Neurobiol. 106–107, 1–16. https://doi.org/10.1016/J.PNEUROBIO.2013.04.001.
Serrano-Pozo, A., Das, S., Hyman, B.T., 2021. APOE and Alzheimer's disease: advances in genetics, pathophysiology, and therapeutic approaches. Lancet Neurol. 20, 68–80. https://doi.org/10.1016/S1474-4422(20)30412-9.
Shiotsuki, H., Yoshimi, K., Shimo, Y., Funayama, M., Takamatsu, Y., Ikeda, K., Takahashi, R., Kitazawa, S., Hattori, N., 2010. A rotarod test for evaluation of motor skill learning. J. Neurosci. Methods 189, 180–185. https://doi.org/10.1016/J.JNEUMETH.2010.03.026.
Siegel, J.A., Haley, G.E., Raber, J., 2010. Apolipoprotein E isoform-dependent effects on anxiety and cognition in female TR mice. Neurobiol. Aging 33, 345. https://doi.org/10.1016/J.NEUROBIOLAGING.2010.03.002.
Simons, M., Krämer, E.M., Macchi, P., Rathke-Hartlieb, S., Trotter, J., Nave, K.A., Schulz, J.B., 2002. Overexpression of the myelin proteolipid protein leads to accumulation of cholesterol and proteolipid protein in endosomes/lysosomes: implications for Pelizaeus-Merzbacher disease. J. Cell. Biol. 157, 327–336. https://doi.org/10.1083/JCB.200110138.
Sinclair, L.I., Love, S., 2017. Effect of APOE genotype on synaptic proteins in earlier adult life. J. Alzheimer's Dis. 59, 1123–1137. https://doi.org/10.3233/JAD-170316.
Sobolewski, M., Anderson, T., Conrad, K., Marvin, E., Klocke, C., Morris-Schaffer, K., Allen, J.L., Cory-Slechta, D.A., 2018. Developmental exposures to ultrafine particle air pollution reduces early testosterone levels and adult male social novelty preference: risk for children's sex-biased neurobehavioral disorders. Neurotoxicology 68, 203–211. https://doi.org/10.1016/j.neuro.2018.08.009.
Southerland, V.A., Brauer, M., Mohegh, A., Hammer, M.S., van Donkelaar, A., Martin, R. V., Apte, J.S., Anenberg, S.C., 2022. Global urban temporal trends in fine particulate matter (PM2·5) and attributable health burdens: estimates from global datasets. Lancet Planet. Health 6, e139. https://doi.org/10.1016/S2542-5196(21)00350-8.
Suades-González, E., Gascon, M., Guxens, M., Sunyer, J., 2015. Air pollution and neuropsychological development: a review of the latest evidence. Endocrinology 156, 3473–3482. https://doi.org/10.1210/EN.2015-1403.
Sun, G.Z., He, Y.C., Ma, X.K., Li, S.T., Chen, D.J., Gao, M., Qiu, S.F., Yin, J.X., Shi, J., Wu, J., 2017. Hippocampal synaptic and neural network deficits in young mice carrying the human APOE4 gene. CNS Neurosci. Ther. 23, 748–758. https://doi.org/10.1111/CNS.12720.
Svenningsson, P., Nishi, A., Fisone, G., Girault, J.A., Nairn, A.C., Greengard, P., 2004. DARPP-32: an integrator of neurotransmission. Annu. Rev. Pharmacol. Toxicol. 44, 269–296. https://doi.org/10.1146/ANNUREV.PHARMTOX.44.101802.121415.
Tanimizu, T., Kenney, J.W., Okano, E., Kadoma, K., Frankland, P.W., Kida, S., 2017. Functional connectivity of multiple brain regions required for the consolidation of social recognition memory. J. Neurosci. 37, 4103. https://doi.org/10.1523/JNEUROSCI.3451-16.2017.
Thier, R., Golka, K., Brüning, T., Ko, Y., Bolt, H.M., 2002. Genetic susceptibility to environmental toxicants: the interface between human and experimental studies in the development of new toxicological concepts. Toxicol. Lett. 127, 321–327. https://doi.org/10.1016/S0378-4274(01)00515-X.
Thompson, J.E., 2018. Airborne particulate matter: human exposure and health effects. J. Occup. Environ. Med. 60, 392–423. https://doi.org/10.1097/JOM.0000000000001277.
Thomson, E.M., 2019. Air pollution, stress, and allostatic load: linking systemic and central nervous system impacts. J. Alzheimer's Dis. 69, 597. https://doi.org/10.3233/JAD-190015.
Traboulsi, H., Guerrina, N., Iu, M., Maysinger, D., Ariya, P., Baglole, C.J., 2017. Inhaled pollutants: the molecular scene behind respiratory and systemic diseases associated with ultrafine particulate matter. Int. J. Mol. Sci. 18, 243. https://doi.org/10.3390/IJMS18020243.
Tuminello, E.R., Han, S.D., 2011. The apolipoprotein e antagonistic pleiotropy hypothesis: review and recommendations. Int. J. Alzheimers Dis. 2011. https://doi.org/10.4061/2011/726197.
van Heuvelen, M.J.G., van der Lei, M.B., Alferink, P.M., Roemers, P., van der Zee, E.A., 2024. Cognitive deficits in human ApoE4 knock-in mice: a systematic review and meta-analysis. Behav. Brain Res. 471, 115123. https://doi.org/10.1016/J.BBR.2024.115123.
Vanbrabant, K., Rasking, L., Vangeneugden, M., Bové, H., Ameloot, M., Vanmierlo, T., Schins, R.P.F., Cassee, F.R., Plusquin, M., 2024. Impact on murine neurodevelopment of early-life exposure to airborne ultrafine carbon nanoparticles. Part Fibre Toxicol. 21, 51. https://doi.org/10.1186/S12989-024-00612-7.
Vandesompele, J., De Preter, K., Pattyn, F., Poppe, B., Van Roy, N., De Paepe, A., Speleman, F., 2002. Accurate normalization of real-time quantitative RT-PCR data by geometric averaging of multiple internal control genes. Genome Biol. 3. https://doi.org/10.1186/gb-2002-3-7-research0034 research0034.1.
Vorhees, C.V., Williams, M.T., 2014. Value of water mazes for assessing spatial and egocentric learning and memory in rodent basic research and regulatory studies. Neurotoxicol. Teratol. 45, 75–90. https://doi.org/10.1016/J.NTT.2014.07.003.
Wang, L., Gui, J., Tian, B., Ding, R., Wang, W., Jiang, C., Zhang, S., Zhang, X., Liu, J., Jiang, L., 2024. Particulate matter induced cognitive impairments via endoplasmic reticulum stress-mediated damage to mitochondria-associated endoplasmic reticulum membranes in immature rats. Toxicology 509, 153979. https://doi.org/10.1016/J.TOX.2024.153979.
WHO, 2005. Air quality guidelines global update 2005 https://doi.org/WHO/SDE/PHE/OEH/06.02.

WHO, 2021. WHO global air quality guidelines [WWW Document]. Particulate matter (PM2.5 and PM10), ozone, nitrogen dioxide, sulfur dioxide and carbon monoxide. URL. https://www.who.int/publications/i/item/9789240034228 (accessed 7.22.25).
Win-Shwe, T.-T., Kyi-Tha-Thu, C., Moe, Y., Fujitani, Y., Tsukahara, S., Hirano, S., 2016. Exposure of BALB/c mice to diesel engine exhaust origin secondary organic aerosol (DE-SOA) during the developmental stages impairs the social behavior in adult life of the males. Front. Neurosci. 9. https://doi.org/10.3389/fnins.2015.00524.
Xie, F., Xiao, P., Chen, D., Xu, L., Zhang, B., 2012. miRDeepFinder: a miRNA analysis tool for deep sequencing of plant small RNAs. Plant. Mol. Biol. 80, 75–84. https://doi.org/10.1007/S11103-012-9885-2.
Yin, R., Tian, F., Frankenberger, B., de Angelis, M.H., Stoeger, T., 2010. Selection and evaluation of stable housekeeping genes for gene expression normalization in carbon nanoparticle-induced acute pulmonary inflammation in mice. Biochem. Biophys. Res. Commun. 399, 531–536. https://doi.org/10.1016/J.BBRC.2010.07.104.
Zannas, A.S., Wiechmann, T., Gassen, N.C., Binder, E.B., 2015. Gene–stress–epigenetic regulation of FKBP5: clinical and translational implications. Neuropsychopharmacology 41, 261. https://doi.org/10.1038/NPP.2015.235.
Zeiss, C.J., 2021. Comparative milestones in rodent and human postnatal central nervous system development. Toxicol. Pathol. 49, 1368–1373. https://doi.org/10.1177/01926233211046933.
Zhang, Y., Pei, Y., Sun, Y., Yang, X., Liang, J., Yin, Z., Liu, Q.S., Zhou, Q., Jiang, G., 2024. AhR agonistic components in urban particulate matter regulate astrocytic activation and function. Environ. Sci. Technol. 58, 4571–4580. https://doi.org/10.1021/ACS.EST.4C00237.

Glossary

AP: Air pollution
AQG: Air quality guideline
AD: Alzheimer's disease
ANOVA: Analysis of variance
apoE: Apolipoprotein E
ASD: Autism spectrum disorder
CNS: Central nervous system
cDNA: Complementary DNA
CNT: Control
Gen: Genotype
HPC: Hippocampus
MWM: Morris Water Maze
NF: Normalization factor
NRQ: Normalized relative quantity
OFT: Open Field Test
PM: Particulate matter
PND: Postnatal day
Cq: Quantification cycle
RQ: Relative quantity
RM-ANOVA: Repeated measures ANOVA
SEM: Standard error of the mean
STR: Striatum
SPT: Sucrose Preference Test
TQ: Target quadrant
TR: Targeted replacement
3CST: Three-Chamber Social Test
Ttm: Treatment
WHO: World Health Organization